Nano Today 57 (2024) 102388

Contents lists available at ScienceDirect

Nano Today

journal homepage: www.elsevier.com/locate/nanotoday

Review

Carbon-based nanomaterials: Multifaceted role in agrochemical recognition, remediation, and release

Vinayak Hegde [a], Mahesh P. Bhat [b,*], Jae-Ho Lee [b], Mahaveer D. Kurkuri [c], Cheol Soo Kim [d], Kyeong-Hwan Lee [a,b,e,**]

[a] Department of Convergence Biosystems Engineering, Chonnam National University, Gwangju 61186, Republic of Korea
[b] AI Agri-Tech Research Center, Chonnam National University, Gwangju 61186, Republic of Korea
[c] Centre for Research in Functional Materials (CRFM), JAIN (Deemed-to-be University), Jain Global Campus, Bengaluru, Karnataka 562112, India
[d] Department of Applied Biology, Chonnam National University, Gwangju 61186, Republic of Korea
[e] BK21 Interdisciplinary Program in IT-Bio Convergence System, Chonnam National University, Gwangju 61186, Republic of Korea

ARTICLE INFO

Keywords:
Agriculture
Carbon nanomaterials
Agrochemicals
Sensing
Remediation
Controlled release

ABSTRACT

Carbon nanomaterials (CNMs) including carbon nanotubes, activated carbon, carbon dots, carbon nanosphere, and graphene, stand out as promising candidates for recognition, remediation, and controlled release of agrochemicals. The structural diversity of these nanomaterials provides exceptional electrical and optical properties, combined with ease of modification, making them attractive materials for enhancing the sensitivity and selectivity of agrochemical sensors. Their large surface-to-volume ratio, porosity, reactive sites, and photocatalytic behavior provide exceptional ability for the sorption and degradation of targeted agrochemicals. Further, to address environmental issues linked to agrochemicals, developing CNM formulations can enable controlled and precise delivery of these chemicals, reducing off-target effects, and bioaccumulation. Their unique features, including nanoscale porous structure, biocompatibility, and altered surface functionalities grant them excellent loading capacity and stimuli-responsive release behavior. Thus, to give insights into the CNMs, this comprehensive review discusses recent advancements in CNM design, the influence of surface functionalities, and properties on selective detection, adsorption/degradation, and release characteristics. However, there is still scope for improving the performance of CNMs by designing composites, providing specific functional sites, and altering surface area. Additionally, applications of a few CNMs are not yet realized despite their promising features, which are highlighted at the end. Finally, the scope for future research directions referring to each application has been discussed to fully realize the potential of CNMs to promote sustainable agricultural practices, paving the way for a healthier and safer environment.

Introduction

As per projections by the United Nations population division, the global population is anticipated to surpass 9.37 billion by 2050 [1]. This growth presents an escalating challenge in ensuring a sufficient supply of nutritious crops [2]. Current estimations of food-demand suggest that to keep pace with the surging demand, crop production must witness a surge of approximately 60–100 % by 2050 [3]. However, plants face numerous challenges, such as unfavorable environmental conditions such as excessive or inadequate soil moisture, extreme weather, environmental pollutants, and nutritional abnormalities [4,5], leading to various plant-related non-infectious diseases. Additionally, pathogens such as fungi, viruses, bacteria, and insects contribute to infectious plant diseases [6,7]. These diseases pose significant threats to plant growth that could result in reduced crop yield [8]. Recent studies suggest that 64 % of the total loss in agricultural yield is due to pests and pathogens [9,10]. To combat plant-related diseases, the agricultural sector heavily relies on various agrochemicals [11], including pesticides and fungicides [12]. In addition, other agrochemicals including herbicides, fertilizers, and plant hormones are also being used for yield management [13–15]. These chemicals help to enhance plant health and growth [16] by mitigating both abiotic and biotic stress [17]. However, conventional

* Corresponding author.
** Corresponding author at: Department of Convergence Biosystems Engineering, Chonnam National University, Gwangju 61186, Republic of Korea.
E-mail addresses: maheshbhat1306@gmail.com (M.P. Bhat), khlee@jnu.ac.kr (K.-H. Lee).

https://doi.org/10.1016/j.nantod.2024.102388
Received 30 December 2023; Received in revised form 11 June 2024; Accepted 28 June 2024

methods of applying agrochemicals have certain limitations including susceptibility to rain drift [18], high organic solvents, poor dispersibility, and bioaccumulation [19,20]. They often result in environmental pollution by generating chemical waste [21], as a significant portion of the chemical disperses into the environment instead of adhering to the plant surface [22]. Improper application of these chemicals can also pose health risks [23] by altering antioxidant and oxidant levels in the human body [12,24].

In this context, the concept of nanotechnology has captured the attention [25] of the research community to recognize [26] and minimize the environmental impact of agrochemicals. The initial step involves the detection of agrochemical wastes to understand their nature and concentrations which allows to implement a remediation strategy [27]. Furthermore, it has paved an avenue for the delivery of these agrochemicals to plants [28], potentially reducing environmental concerns [12]. By adopting nanotechnology, agricultural practices can become more efficient, sustainable [29], and environmentally friendly, ensuring the production of healthier crops, and minimizing adverse side effects on human health and the ecosystem [30]. A variety of nanomaterials such as polymers [31], silica, hydrogels, metal-organic frameworks (MOFs), layered double hydroxides (LDH), and carbon nanomaterials (CNMs), are being used in numerous agriculture-related applications, primarily focusing on sensing, remediation, and delivery [15,32].

Carbon, a non-metal abundant in the biosphere, exhibits remarkable versatility due to its ability to exist in allotropic forms ranging from 0-D to 3-D structures [33]. Due to diverse orbital hybridization, carbon can form various chemical bonds with different orientations [34], enabling the creation of a variety of CNMs with superior physical and chemical properties [35]. CNMs have shown considerable potential due to their desirable properties, including uniform dispersion, low toxicity, superior biocompatibility, stable molecular structure, optical properties [36], exceptionally high surface area [37], and porosity that enables them to be used in a variety of research fields [32,38]. The pivotal discovery of the first-ever CNM, fullerene, in 1985 [39] paved the way for subsequent research and exploration in the field of carbon nanomaterials (Fig. 1**a**). The invention of carbon nanotubes (CNTs) and graphene further heightened interest in the remarkable properties and potential applications of CNMs [40]. Here, we have made an effort to highlight the progressive history of different CNMs in sustainable agriculture with the first-ever report irrespective of their applications (Fig. 1**b**). Accounting for 40 % of all nanotechnology-related applications in agriculture, CNMs contribute significantly to modern agricultural practices [41]. CNMs demonstrate lower detection levels for target analytes due to their large surface area and porosity, possessing a high density of active sites [42], which improve both selectivity and reactivity. Further, with inherent adsorption and photocatalytic properties, CNMs have been proven to be efficient in pollution remediation [43]. The removal performance of CNMs is associated with their composition and surface functionality, which can be enhanced as well as reinforced by functionalizing them in the presence of acid and alkali mediums, thereby achieving better chemical reactivity towards target pollutants [44,45]. Furthermore, the sp^2-hybridised CNMs are generally

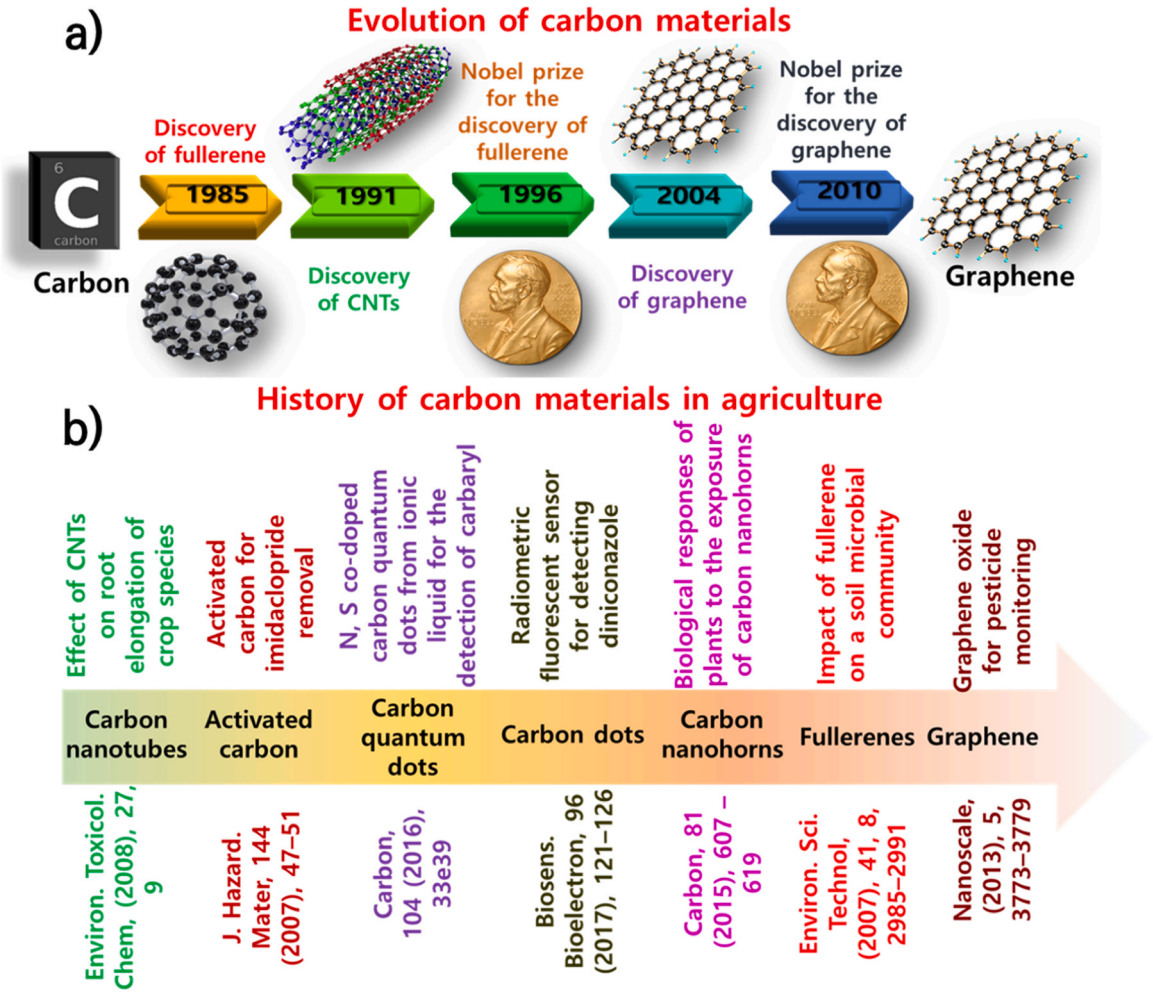

Fig. 1. a) Evolution of CNMs over the past years with major milestones from fullerenes to the groundbreaking debut of graphene. b) Progressive history of CNMs with first ever reported research work in the field of agriculture.

considered nontoxic and biocompatible at adequate doses [46] and are considered a promising platform for the delivery of agrochemicals at plant cellular level. Also, their excellent heat conversion capacity in the near-infrared (NIR) region could facilitate photothermal performance (PTT) [47]. The exceptional physicochemical stability and supramolecular π-π stacking enable the high loading capacity and controlled release [48]. Thus, CNMs can be considered the next generation of delivery platforms in agricultural practices.

Thus, in this comprehensive review, we intend to provide information on the latest advancements of CNMs in environmental and agricultural-related applications. The review is structured into three major sections: (i) CNMs for agrochemical sensing, (ii) agrochemical remediation, and (iii) agrochemical delivery. Further, synthesis, surface modification of CNMs, the fabrication of sensors, sensing mechanisms, sensitivity and selectivity, maximum adsorption/removal efficiency, photodegradation efficiency, loading efficiency, stimuli-responsive release mechanisms, their application efficacy, and impact of the CNMs on the plant is discussed. Additionally, a discussion on potential opportunities and future research directions for each application category of CNMs is provided. Finally, we believe that by exploring and harnessing the full potential of CNMs, the agricultural sector can achieve greater sustainability and productivity in the future.

Carbon nanomaterials for agrochemical sensing

Addressing the environmental contamination and health risks associated with excessive agrochemical use necessitates a systematic approach to monitor their presence in the environment. Traditional analytical methods such as high-performance liquid chromatography (HPLC), gas chromatography (GC) [49], enzyme-linked immunosorbent assay (ELISA) [50], and electrochemical assay [51] are used for detecting pollutants in the ecosystem. However, they have limitations including high costs, time-consuming sample preparation, and the need for skilled operators [52]. Hence, there is a requirement for alternative, sensitive, and rapid sensing probes that can meet the practical demands of environmental monitoring [53–55]. Recently, CNMs-based sensing probes have emerged as promising solutions due to their unique properties such as exceptional binding capabilities, large surface area, minimal residual current, wide potential window, rapid electron transfer, renewable surface features, optical, and fluorescent characteristics [56]. The large surface area of CNMs allows for increased interaction with pollutants [57], enhancing the sensitivity to detect even trace levels of contaminants. The surface of CNMs can be modified with different functional groups for selective detection of specific pollutants. The high electrical conductivity, which varies in the presence of certain pollutants, allows for the development of sensitive sensors [58]. These advancements in nanotechnology-based sensing systems have great potential to improve environmental monitoring practices, contributing to a safer and healthier ecosystem.

Carbon nanotubes (CNTs)

Organophosphorus compounds (OP), which make up 30–40 % of global pesticides, are major pollutants [59] that can accumulate in the human body and potentially cause problems in the respiratory and nervous system [60]. CNTs have emerged as an attractive solution for the electrochemical detection of agrochemicals due to their large surface area and broad potential window of −1.0 to +1.0 V, allowing for a wide range of redox reactions [61]. In a recent study glassy carbon electrode (GCE) was modified with ink containing nitrogen-sulfur co-doped

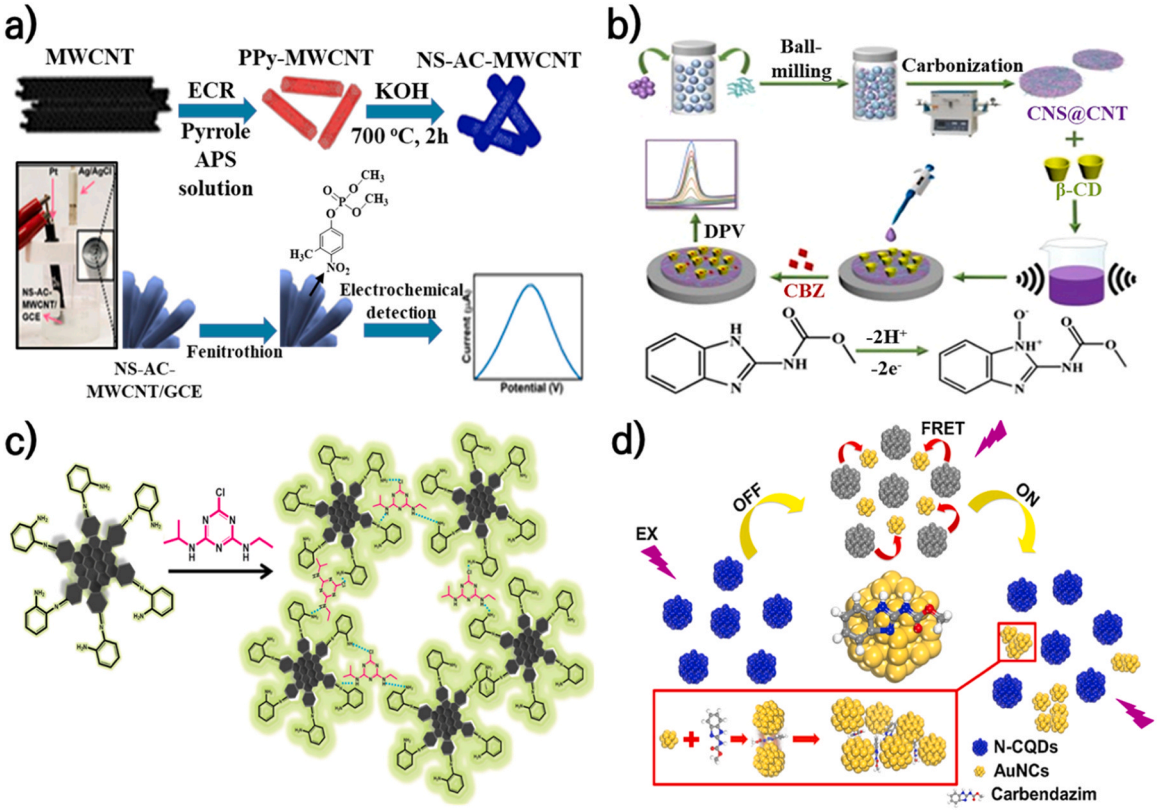

Fig. 2. Schematic representation of a) synthesis of NS-AC-MWCNT through KOH activation of PPy-coated MWCNTs and sensor fabrication by modifying GCE with NS-AC-MWCNT. b) Fabrication of β-CD/CNS@CNT/GCE sensor for the detection of carbendazim. c) Plausible aggregation of oPCD in the presence of atrazine. d) N-CQDs/AuNCs as fluorescence turn-on sensor for carbendazim.
(a) Printed with permission from Ref. [62]. Copyright 2021, American Chemical Society. (b) Printed with permission from Ref. [65]. Copyright 2022, Elsevier. (c) Printed with permission from Ref. [69]. Copyright 2018, Elsevier. (d) Printed with permission from Ref. [72]. Copyright 2019, Elsevier.

activated carbon-modified multi-walled carbon nanotubes (NS-AC-MWCNT) for the electrochemical detection of fenitrothion (FT) a phosphorothioate insecticide [62] (Fig. 2a). The electrode's performance was enhanced by coating MWCNTs with polypyrrole (PPy) and activated carbon (AC), increasing surface area and electrical conductivity. This modified electrode demonstrated high sensing capabilities for FT, achieving a limit of detection (LoD) of 4.91 nM. Selectivity tests showed a 10-fold excess concentration of common salts and OPs did not affect the performance. The sensor was successfully used to detect FT in real environmental samples, including lake and tap water, with recovery rates of 86.4 % ± 8.2 % and 96.9 % ± 2.0 %, respectively. Further studies on the sensor's long-term stability and reproducibility are needed to better understand its robustness and reliability for on-site applications.

OPs can irreversibly bind to the acetylcholinesterase (AChE) enzyme, inhibiting its activity and leading to an accumulation of the neurotransmitter acetylcholine in the human body [63]. This has led to the development of AChE-functionalized sensors. In this context, a biosensor for detecting paraoxon was developed by doping AChE through an amide bond onto the surface of GCE coated with carboxylic groups modified MWCNTs [64]. The presence of AChE enzyme functioned through an inhibition mechanism and exhibited a LoD of 0.1 nM. Despite the presence of interferents such as sugars, inorganic ions, nitrophenyl derivatives, and electroactive species, the biosensor showed selectivity for paraoxon. However, when used to detect paraoxon in real-world samples like tap water and potatoes, the biosensor showed slightly altered enzyme inhibition compared to buffer solutions, indicating a limitation in accurate quantification. This deviation might be due to the use of a glass slide instead of a GCE. Future research could focus on optimizing the sensor design to minimize interferences from sample matrices, ensuring consistent and reliable detection.

Understanding the impact of different forms of carbon materials on CNTs is crucial to enhancing their sensing capabilities. In this regard, carbon nanosheets (CNS) were integrated with CNTs (CNS@CNT) functionalized with β-cyclodextrin (β-CD) to enhance the sensitivity of carbendazim (CBZ) detection at pH 7 (Fig. 2**b**) [65]. The sensor's sensitivity for CBZ was attributed to the large surface area, electrical conductivity of CNS, and superior host-guest supramolecular recognition ability of β-CD. The β-CD helped to prevent sensor composite aggregation and facilitated CBZ selectivity, achieving a LoD of 9.4 nM. Despite a 100-fold excess concentration of various inorganic salts and an equal concentration of other compounds, the sensor maintained its selectivity towards CBZ. The sensor showed a satisfactory recovery rate of 97.1 % - 99.4 %, demonstrating its reliability. However, the study primarily focused on the detection of CBZ in apple juice, which limits the sensor's applicability to other sample matrices.

Carbon quantum dots (CQDs)

CQDs have gained attention in sensing and bioimaging due to their easy synthesis, high photoluminescence quantum yield (PLQY), remarkable photostability, and versatile luminescent properties [66]. Their sensing mechanism is based on the quenching of their photoluminescence due to aggregation, electron/energy transfer, or the revival of fluorescence within pre-quenched CQD-quencher complexes [67], which makes CQDs suitable for detecting various agrochemicals. Triazines, a class of agrochemicals, are of concern due to their low solubility, slow degradation, high stability, and potential risks such as carcinogenicity, hormone disruption, and immune suppression [68]. To address this, a fluorescent sensor was developed using CQDs derived from ortho-phenylenediamine (oPCD) for detecting the triazine-based herbicide, atrazine (ATZ) in real samples like lemon, sugarcane, and cucumber [69]. The sensor forms hydrogen bond with ATZ through the amine groups on its surface, inducing the aggregation of CQDs and augmenting fluorescent luminosity (Fig. 2c). The sensor demonstrated a LoD of 3 pM, indicating high sensitivity. Its exceptional cell permeability and emission strength within bacterial cells make it promising for real-time sensing of ATZ through bioimaging. The sensor remained sensitive to ATZ even in the presence of other pesticides and some cations. Its ability to function effectively in living cells opens up an avenue for exploring the presence of agrochemicals at the cellular level, expanding its potential applications in environmental and biomedical research.

CBZ used as a preservative in orange cultivation [70], has strong soil adsorption and chemical stability, allowing it to persist in the environment. However, it can negatively affect liver health and spermatogenesis in mammals [71]. Thus, a fluorescent sensor was developed to detect CBZ, using a nanohybrid of nitrogen-doped carbon quantum dots (N-CQDs) and gold nanoclusters (AuNCs) [72]. A strong fluorescence resonance energy transfer (FRET) was observed between the N-CQDs and AuNCs. When CBZ was introduced, the interaction between the N-CQDs and AuNCs reduced, leading to AuNCs aggregation and recovery of the fluorescence properties, with a LoD of 0.83 μM (Fig. 2d). The sensor's selectivity was tested with various cations and other pesticides, revealing slight interference from these substances, however, only CBZ significantly enhanced the fluorescence intensity. However, the study lacks information on the sensor's long-term stability and reproducibility, and potential interferences from other co-existing compounds with CBZ, which could affect CBZ detection accuracy, limiting its real-world applications.

The integration of CQDs into other solid host materials has shown excellent fluorescence properties and improved stability in solutions [73]. In this context, a dual sensing strategy was developed by introducing CQDs derived from oPCD into the channels of (Zr)-UiO-66-NH_2 MOF to detect quinalphos pesticide in the presence of copper (Cu^{2+}) ion [74]. The sensor exhibited a LoD of 0.5 μM for Cu^{2+} and 0.3 nM for quinalphos, the lowest reported value among similar studies. The sensing capabilities of the sensor can be attributed to the synergetic features of the porous structure of the UiO-66-NH_2, which enhances pesticide adsorption, and the luminescent properties of the CQDs. Upon the introduction of Cu^{2+} ions, the fluorescence of the sensor diminished due to the binding interaction between UiO-66-NH_2 and Cu^{2+}. However, in the presence of quinalphos, the fluorescence of sensor was restored, likely due to the binding of Cu^{2+} ions with quinalphos, leading to the release of the CQDs-UiO-66-NH_2 into the surrounding medium (Fig. 3a). A significant limitation of this approach is that the detection of quinalphos is dependent on the presence of Cu^{2+} ions.

In recent years, the development of biomaterial-derived eco-friendly and cost-effective sensors has attracted the interest of the research community. With this aspect, jatropha fruit-derived CQDs (J-CQDs) were synthesized using a hydrothermal method for the detection of OP, specifically chlorpyrifos [53]. The detection strategy was based on the irreversible catalytic inhibition of the AChE enzyme, which is monitored by the decrease in the fluorescent intensity of J-CQDs at 462 nm. The process involves the hydrolysis of acetylthiocholine (ATCh) by AChE, producing thiocholine (TCh) which causes 5,5-dithiobis (2-nitrobenzoic acid) (DTNB) to decompose and form yellow colored 2-nitro-5-thiobenzoic acid (TNBA). The addition of J-CQDs causes TNBA to quench the fluorescence emission spectra of J-CQDs. The catalytic activity of AChE was reduced by chlorpyrifos, resulting in the recovery of the fluorescence signal. The probe demonstrated a LoD of 2.7 ng mL^{-1}, with a linear detection range from 0.02 to 0.18 g mL^{-1}. The selectivity studies revealed that the presence of several metal ions and biomolecules did not affect the fluorescence emission of J-CQDs. The probe exhibited a recovery rate from 93.3 % to 100 % for river water and apple juice samples, indicating its potential for practical use in environmental monitoring and pesticide detection.

Graphene

The use of functionalized graphene materials, including graphene quantum dots, graphene oxide, and reduced graphene oxide, has

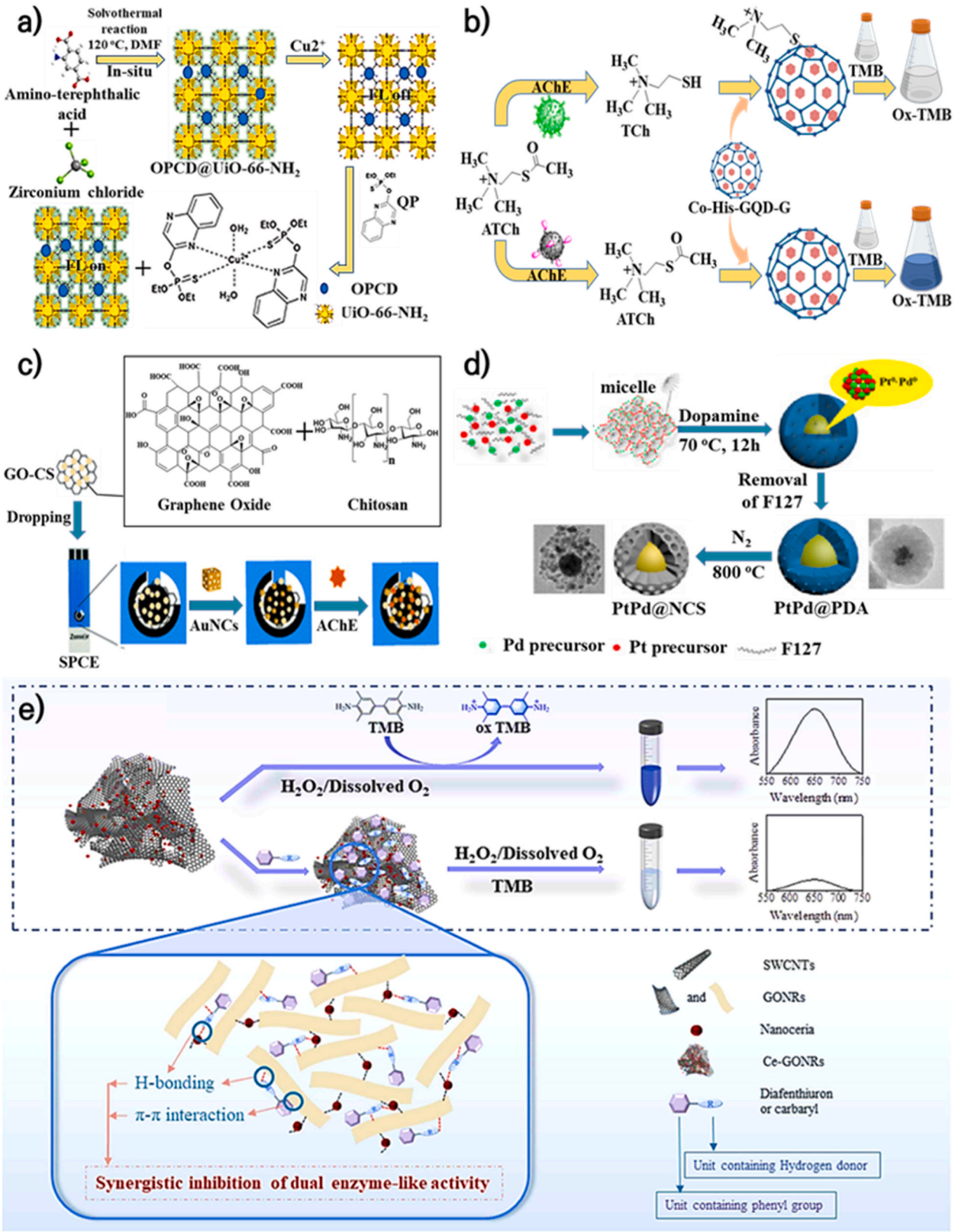

Fig. 3. Schematic representation of a) synthesis of CQD@UiO-66-NH_2 through the solvothermal method and sensing mechanism of quinalphos. b) Colorimetric detection of chlorpyrifos using Co-His-GQD-G by oxidation of TMB to ox-TMB. c) Development of AChE biosensor-based GO-CS and AuNC nanocomposite for the detection of chlorpyrifos. d) Designing of PtPd@NCS core-shell nanocomposite sensor through the in-situ hydrothermal process. e) Colorimetric detection mechanism for diafenthiuron and carbaryl involving π-π stacking and hydrogen bonding interactions between insecticide and Ce-GONRs.
(a) Printed with permission from Ref. [74]. Copyright 2021, Elsvier. (b) Printed with permission from Ref. [80]. Copyright 2021, Elsvier. (c) Printed with permission from Ref. [81]. Copyright 2019,The Royal Society of Chemistry. (d) Printed with permission from Ref. [86]. Copyright 2018, Elsevier. (e) Printed with permission from Ref. [84]. Copyright 2022, Elsevier.

enabled the creation of a wide array of highly sensitive sensors encompassing colorimetric, electrochemical, potentiometric, and fluorescence probes [75]. The combination of functional groups with graphene yields remarkable features, including enhanced sensitivity that allows for the detection of low concentrations of target analytes, specificity without cross-reactivity, rapid results, cost-effectiveness, prolonged shelf life, robust stability, and ease of use [76]. The detection of OP is of importance due to its harmful effects on human health [77]. Given the distinctive characteristics of graphene, there is a compelling interest in assessing its efficacy for real-time detection of agrochemicals [78]. Among various sensing techniques, colorimetric sensors are particularly notable for their ability to identify analytes visually [79]. However, achieving high sensitivity in analyte detection using this method is a significant challenge. In a relevant study, a hybrid system (Co-His-GQD-G) that uses cobalt nanocrystals on histidine-functionalized graphene quantum dots and graphene oxide composites to detect chlorpyrifos in the peaches was developed (Fig. 3**b)** [80]. The sensor demonstrated oxidase-like activity and quasi-superparamagnetic behavior, achieving a LoD of 0.57 ng mL^{-1}. The presence of chlorpyrifos enhanced the catalytic activity of Co-His-GQD-G toward oxidation of 3,3′,5,5′-tetramethylbenzidine (TMB) to ox-TMB, leading to a color change to dark blue. The sensor's performance was not significantly affected by other substances found in peaches up to a concentration of 20 ng mL^{-1}. However, a major drawback of this study is the longer optimized incubation time of 40 min to achieve maximum sensitivity. Continuing with the aforementioned studies on OP detection introduced a biosensor combining graphene oxide (GO), gold nanocages (AuNC), and chitosan (CS) for chlorpyrifos detection (Fig. 3**c)** [81]. This distinctive design leverages the advantages of the dual effective surface and the highly porous structure of Au nanocages, coupled with the large surface area offered by GO. The inclusion of CS plays a pivotal role in ensuring the stability of the biosensor. Additionally, AChE was immobilized to enhance the electrocatalytic activity of the biosensor, achieved a LoD of 3 ng L^{-1}, benefiting from the material's electrical conductivity and surface area, which enable faster electron transfer and high sensitivity. The longer AChE inhibition time of 12 min to detect chlorpyrifos and lack of interference studies for other OPs are the major limitations of this study.

Further, a biosensor was designed to detect carbaryl (carbamate class insecticide) in food. Carbamates, like OPs, inhibit the AChE enzyme, which is critical for nerve function [82]. Herein, an electrode was fabricated from reduced graphene oxide (rGO) and AChE layered onto GCE [83]. The biosensor achieved a LoD of 1.9 nmol L^{-1} and was able to detect carbaryl in tomato samples at a level of 0.47 ± 0.04 μmol L^{-1}. Furthermore, differential pulse voltammetry (DPV) tests using glyphosate did not affect the oxidation process of thiocholine, suggesting the biosensor's selective response to carbaryl. However, the study did not explore the other potential interfering agrochemicals in complex food matrices. Another study explored a colorimetric sensor for detecting the pesticides diafenthiuron and carbaryl [84]. The sensor utilized porous cerium-doped GO nanoribbons (Ce-GONRs), which have dual enzyme-like activities that can catalyze the oxidation of TMB, a chemical used in colorimetric assays. The sensor's porous structure contributed to high selectivity, effectively distinguishing between diafenthiuron and carbaryl. The interaction between the pesticides and the Ce-GONRs, through π-π stacking and hydrogen bonding, inhibited the Ce-GONRs' enzyme-like activities with LoD of 0.57 ng L^{-1} and 0.23 ng L^{-1} for diafenthiuron and carbaryl, respectively (Fig. 3**e**). The sensor showed strong selectivity for these two pesticides, with a concentration of 1 μg mL^{-1} sufficient to inhibit its catalytic activity. In contrast, 19 other common pesticides had a negligible effect even at 5 μg mL^{-1}. However, thiram did cause slight inhibition, which is a noted limitation of the sensor.

Other carbon nanomaterials

Core-shell carbon structures are of significant interest in the research community, due to their immense potential across various domains. Recent investigations have unveiled that core-shell metal@carbon nanostructures containing nickel (Ni) and cobalt (Co), showcase remarkable electrochemical characteristics while effectively preventing agglomeration [85]. A nanocomposite with a bimetal core surrounded by an N-doped carbon shell **(**AChE/PtPd-NCS/GCE) was developed to detect OPs (Fig. 3**d)** [86]. This composite was synthesized using dopamine as a reducing agent in conjunction with carbon and nitrogen sources through a hydrothermal process. The electrochemical performance of the sensor was ascribed to their porous structure, for rapid electron transfer, and a synergistic effect from the N-doped carbon, platinum, and palladium. The sensor exhibited a LoD of 7.9×10^{-15}, 8.6×10^{-15}, and 7.1×10^{-14} M for malathion, parathion methyl, and chlorpyrifos, respectively. The detection mechanism was attributed to blocking AChE's serine hydroxyl groups with insecticides, reducing AChE activity through covalent bond formation. Further, the DPV response for the sensor in the presence of interferents showed no considerable changes in the current response. However, the detection was interfered with an equal quantity of pesticides like carbaryl and chlorpyrifos.

Recently, carbon nanospheres (CNS) have gained attention as a promising material for enhancing electrochemical sensors due to their chemical stability, conductivity, and surface area. Considering CNS cost-effectiveness and stable dispersion, an electrochemical sensor for detecting the herbicide bentazon (BTZ) was developed using CNS-modified GCE crosslinked with chitosan films (CNS-CTS-ECH/GCE) [87]. The use of epichlorohydrin (ECH) as a cross-linker improved the analytical signal and electron transfer properties. The sensor's electrooxidation process for BTZ involves a single electron transfer and subsequent dimerization of the oxidation product with a LoD of 1.4 μM L^{-1} and sensitivity of 6.22 A mol^{-1} Lcm^{-2}. The sensor showed selectivity in the presence of other cations and agrochemicals with relative standard deviation (RSD) values below ± 9 %. However, the study did not examine the effect of pH on detection or the sensor's performance in complex environmental samples other than water, which could affect its practical field application.

To achieve an electrochemically active surface area and rapid electron transfer capability, a gadolinium oxide functionalized carbon nanospheres modified GCE (Gd_2O_3/f-CNS/GCE) was developed for the detection of CBZ, achieving a LoD of 0.009 μM L^{-1} [88]. This sensitivity is due to the electrode's large surface area, high electron conductivity, and numerous adsorptive sites, which also led to an enhanced anodic peak current. The sensor exhibited < 10 % relative error even with significant excesses of other compounds. However, the study did not address the impact of analyte pH on detection, which is a potential limitation for real-time applications. Further, a study focused on hollow bowl-like carbon (HBC) materials, known for their lower symmetry and open structure, are instrumental in increasing the loading density and reducing charge transfer distance, which leads to an efficient and quick response. An N-dopped HBC (NHBC) composite was examined for CBZ detection, showing a LoD of 2.7 nM and a broad linear range from 0.005 to 8.0 μM [89]. The introduction of N-doping in NHBC creates more defects and abundant active sites, thereby enhancing the electro-analysis performance of the sensor. The high sensitivity was attributed to the NHBC's cavity structure, which allows for volume expansion and closer electron transfer. Moreover, NHBCs facilitate an increased utility ratio of the internal surface, offering more active sites and areas to accumulate CBZ molecules. Tests for selectivity against various ions and pesticides confirmed the sensor's excellent anti-interference capabilities, with no significant changes in peak current values.

The above studies illustrate the advancements in agrochemical detection using carbon-based sensors. CNMs have been designed with

Table 1
Agrochemical sensing performance of different carbon-based sensor materials with their target agrochemicals and limit of detection.

Sensor material	Target agrochemical	Limit of detection	Ref.
NS-AC-MWCNTs	Fenitrothion	4.91 nM	[62]
AChE/MWCNTs	Paraoxon	0.1 nM	[64]
CNS@CNT	Carbendazim	9.4 nM	[65]
CQDs	Atrazine	3 pM	[69]
N-CQDs/AuNCs	Carbendazim	0.83 μM	[72]
CQDs@UiO-66-NH_2	Quinalphos	0.3 nM	[74]
J-CQDs	Chlorpyrifos	2.7 ng mL^{-1}	[53]
Co-His-GQD-G	Chlorpyrifos	0.57 ng mL^{-1}	[80]
NCs/GO–CS/AChE/SPCE	Chlorpyrifos	3 ng L^{-1}	[81]
rGO/AChE	Carbamate	1.9 nmol L^{-1}	[83]
Ce-GONRs	Diafenthiuron	0.57 ng L^{-1}	[84]
	Carbaryl	0.23 ng L^{-1}	
AChE/PtPd-NCS/GCE	malathion, parathion methyl, and chlorpyrifos	7.9×10^{-15}, 8.6×10^{-15}, 7.1×10^{-14} M	[86]
CNS-CTS-ECH/GCE	Bentazon	1.4 μ mol L^{-1}	[87]
Gd_2O_3/f-CNS/GCE	Carbendazim	0.009 μM L^{-1}	[88]
NHBC	Carbendazim	2.7 nM	[89]

Table 2
Different carbon-based adsorbent materials and their target agrochemical pollutants with removal efficiencies.

Adsorbent material	Target pollutant	Removal efficiency	Ref.
ZIF-8/MWCNTs	Diazinon, Triazophos, Profenofos, Phosalone, Ethoprop, Methidathion, isazofos, and Sulfotep	2.59, 3.12, 3.89, 3.80, 2.18, 2.34, 3.00, 2.84 mg g^{-1}	[94]
f-MWCNTs/PVA	Diazinon, Chlorpyrifos, Pirimiphos-methyl, and Malathion	98–99 %	[95]
MCNTs	Diazinon	98.5 %	[96]
MWCNT/MPNs-Fe	Glyphosate	43.66 mg g^{-1}	[97]
ZIF-8@MPCA and UiO66-NH_2@MPCA	Chipton, Alachlor and Chipton, Alachlor	160.9 mg g^{-1}, 246.8 mg g^{-1} and 196.2 mg g^{-1}, 232.8 mg g^{-1}	[98]
CNT/Fe_3O_4	Pirimicarb	101.3 mg g^{-1}	[99]
GAB	4-Chloro-2-methyl phenoxy acetic acid, 2,4-Dichlorophenoxy acetic acid	599.8785 mg g^{-1} 367.1519 mg g^{-1}	[101]
CPB	4-Chloro-2-methyl phenoxy acetic acid, 2.4-Dichlorophenoxy acetic acid	399.865 mg g^{-1} 273.0683 mg g^{-1}	[101]
Activated carbon	Bendiocarb	7.97 mg g^{-1}	[103]
	Metolcarb	9.11 mg g^{-1}	
	Isoprocarb	13.95 mg g^{-1}	
	Pirimicarb	39.37 mg g^{-1}	
	Carbaryl	44.64 mg g^{-1}	
	Methiocarb	93.46 mg g^{-1}	
Activated carbon	2,4-Dichlorophenoxyacetic	367.77 mg g^{-1}	[104]
MnF_2O_4 @AC	Acetochlor	226 mg g^{-1}	[105]
Activated carbon fabric	Metaldehyde	1375 μg g^{-1}	[106]
MGO-NGC	Chlorpyrifos	78.74 mg g^{-1}	[108]
	Hexaconazole	93.4 mg g^{-1}	
AGu@mGO	Chlorpyrifos	85.47 mg g^{-1}	[111]
AFG@30MIL-101(Fe)	Diazinon	100±1 %	[115]
	Atrazine	81±1 %	
GO-$CoFe_2O_4$	Acetamiprid	97 %	[116]
TiO_2/$GO_{7\ \%}$	2,4-D	100 %	[94]

tailored receptors to effectively interact with specific agrochemical targets, allowing for the detection at lower concentrations. These sensors offer rapid response times and the ability for real-time monitoring of

Table 3
Carbon nanocarriers and their delivery agrochemicals with loading and releasing capacity.

Carrier material	Delivery agrochemical	Loading efficiency	Cumulative release %	Ref.
MWCNTs	Pyraclostrobin	16.64 %	86.7	[125]
N-doped activated carbon	(2,4-D) sodium	21.50 %	48	[128]
γ-FeOOH@BC	Quinclorac	90 mg g^{-1}	88	[129]
GO@$Cu_{2-x}Se$	Chlorpyrifos	40 %	30	[133]
PLA/GO	Pyraclostrobin	39.89 %	98	[134]
GO	Pyraclostrobin	87.04 %	70	[136]
PNIPAm-GO	Lambda-cyhalothrin	15.4 %	54.9	[137]
PEG-GO	Emamectin benzoate	164.7 %.	36.5	[140]
Graphene oxide	Abamectin	-	32	[141]
CMC/CNPs	Emamectin benzoate	55.56 %	76	[143]
HCM/IMI/PEG/ α-CD	Imidacloprid	-	77	[144]
Carrier material	**Fertilizers**	**Observed result**		**Ref.**
MWCNTs	Urea (N-fertilizer)	NU: 1363 mg/pot and NUE: 96.35 % in paddy for 21 h		[148]
Biochar	Urea (N-fertilizer)	65.28 % of N leaching in 22 days		[149]
Biochar hydrogel	Nitrogen (N), Phosphorus (P), and Potassium (K)	Controlled release rate < 85 % in 12 days		[150]
Biochar	Urea	Release of 45–70 % during the first hour, followed by the slow release until the end of 72 h		[151]
γ-FeOOH/BC	Phosphate	Release rate of 13.68 % at pH 2, 88 % at pH 11, and 92 % at 35 °C		[129]

agrochemical residues. Despite these advantages, there is a need for more efficient, sensitive, and selective sensing platforms for on-site agrochemical detection. Such innovative platforms could be instrumental in promoting sustainable agricultural practices. Carbon nanohorns, fullerenes, and activated carbons are rarely explored for sensing applications, due to the lack of inherent optical, electrical, sensitive, and selective properties. However, there is potential for these materials to be adapted for future sensor applications through surface modification and integration with other nanomaterials.

Carbon nanomaterials for agrochemical remediation

The inappropriate use of agrochemicals emerged as a significant factor contributing to environmental pollution, posing detrimental effects on life and water bodies [90]. Thus, the below section aims to elucidate the use of CNMs for the efficient removal of agrochemical wastes through adsorption and degradation methods, owing to their low cost, ease of regeneration, and high efficiency. The use of carbon for water purification is not new; it dates back to 450 BC with charcoal filters, and in 1773, Scheele's observation of charcoal's adsorptive properties led to the widespread use of activated carbon for water treatment [91]. In past decades, CNMs have been engineered with functional groups to improve their chemical interactions, thus enhancing their adsorption and degradation capabilities. Unlike other NPs, CNMs are considered to be eco-friendly as they are derived from

natural sources [92], and they offer efficient removal without introducing additional contaminants.

Carbon nanotubes (CNTs)

CNTs are increasingly used as adsorbents to capture a wide range of environmental pollutants due to their abundant active sites, distinctive hollow structures, and strong affinity for pollutants [93]. However, CNTs have certain limitations such as agglomeration and reduced adsorption efficiency towards some OPs. To address this, a hybrid ZIF-8 modified magnetic MWCNTs was synthesized through an in-situ chemical coordination method (Fig. 4**a**) [94]. The coordination-polymerization process facilitated the decoration of ZIF-8 onto the surface of MWCNTs, resulting in a specific surface area (SSA) of 127.95 m^2 g^{-1}. The adsorbent was utilized for the remediation of eight different pesticides such as diazinon, triazophos, profenofos, phosalone, ethoprop, methidathion, isazofos, and sulfotep. The maximum adsorption capacities (q_e max) for these pesticides were found to be 2.59, 3.12, 3.89, 3.80, 2.18, 2.34, 3.00, and 2.84 mg g^{-1}, respectively. The adsorption performance can be attributed to the superparamagnetic nature of MWCNTs, high porosity of the ZIF-8 MOF, and valence electron driven adsorption through sharing of electrons between pesticides and ZIF-8@MWCNTs. However, the q_e max was lower than some previously reported literatures, possibly due to lower SSA and competitive adsorption among the pesticides. Thus, solvothermal deposition of ZIF-8 on the MWCNTs could promote the controlled growth of MOF, thereby enhancing the surface area and porosity.

Earlier studies suggested that the properties of CNTs can be improved by combining them with synthetic polymers. For instance, MWCNTs functionalized with chlorine (Cl) and integrated into polyvinyl alcohol (PVA) matrix showed high adsorption efficiency against OPs such as diazinon, chlorpyrifos, pirimiphos-methyl, and malathion [95]. The MWCNT was acid treated followed by thionyl chloride ($SOCl_2$) treatment to introduce carboxylic acid (-COOH) groups to facilitate the functionalization of Cl. Further, PVA was crosslinked with Cl functionalized MWCNTs using citric acid to obtain nanocomposite films. The film demonstrated swelling behavior and removed 98–99 % of tested pesticides. Despite their removal efficiency, the adsorbent's selectivity for specific pollutants remains a challenge, as cross-interference from various pesticides in real samples could affect its performance. Furthermore, MWCNTs with a SSA 370 m^2 g^{-1} were shown to completely remove diazinon (class of OP) from water at an initial concentration of 0.3 mg L^{-1} [96]. Upon testing with real water samples containing diazinon at natural pH levels, the MWCNTs exhibited a removal rate of 98.5 %. Nonetheless, higher concentrations of pesticides could lead to reduced adsorption due to particle aggregation. To tackle this issue, modifying the MWCNTs surface with additional functionalities holds the potential to enhance performance and stability in more

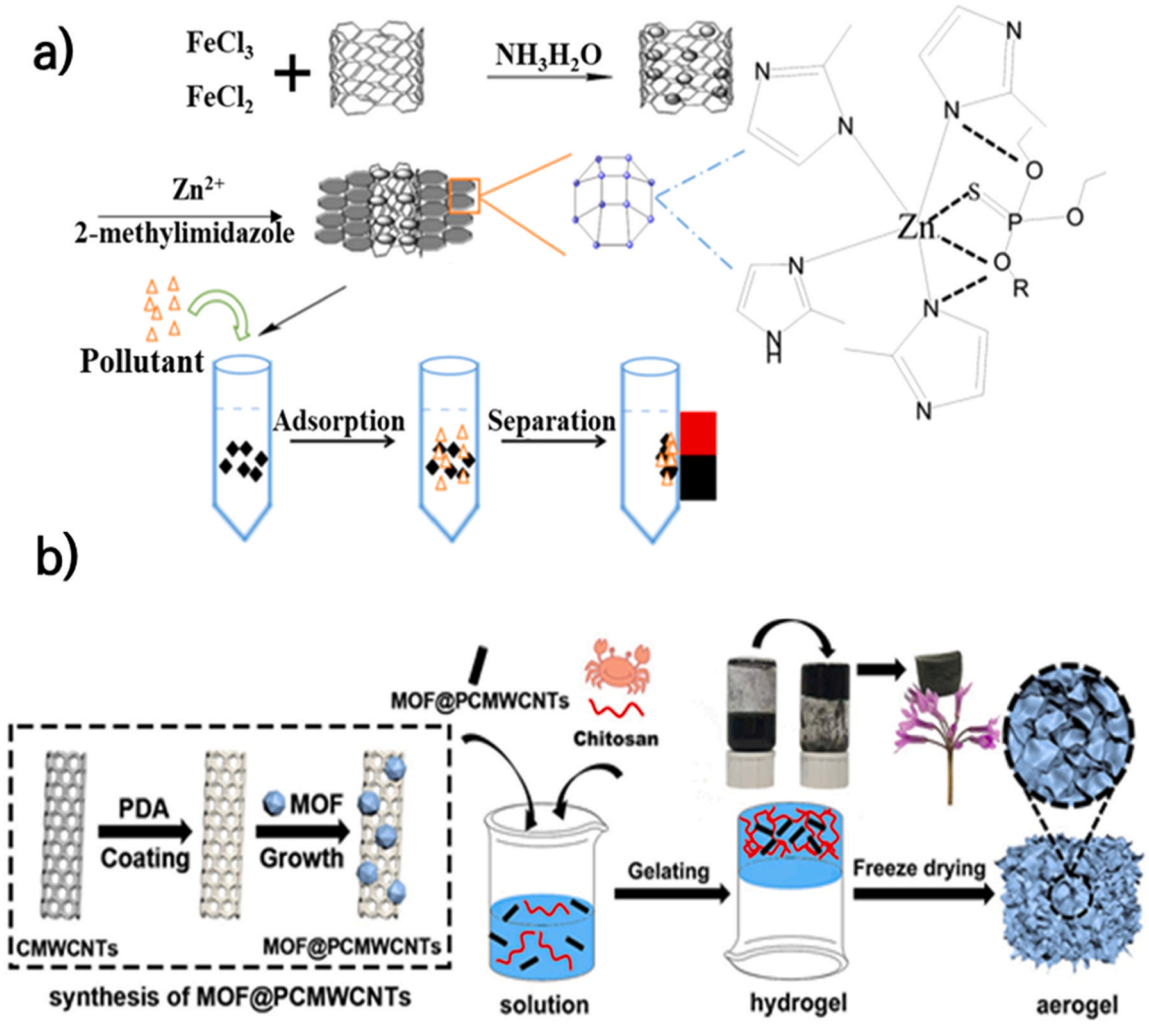

Fig. 4. Schematic representation of a) preparation of ZIF-8@MWCNT adsorbent material and adsorption mechanism with model pesticides. b) Synthesis of aerogel adsorbent by MOF particle-modified MWCNT (ZIF-8@MPCA and UiO-66-NH_2@MPCA).
(a) Printed with permission from Ref. [94]. Copyright 2019, Elsevier. (b) Printed with permission from Ref. [98]. Copyright 2020, Elsevier.

challenging environmental conditions. This approach not only addresses limitations but also underscores the versatility and adaptability of MWCNTs as promising adsorbents for pesticide removal.

To evaluate the efficiency of surface-modified MWCNTs, a study was conducted on the removal of glyphosate using MWCNT impregnated with metallic nanoparticles (MWCNT/MPNs-Fe), synthesized through a green method using plant extracts [97]. This synthesis approach prevented the NP aggregation, as the phytochemical contents acted as a coating agent. The resulting adsorbent exhibited a SSA of 94 $m^2\ g^{-1}$ and a pore diameter of 20 nm, with a maximum adsorption capacity of 43.66 mg g^{-1} within 120 min. The adsorbent demonstrated 68.38 % and 40.33 % removal in the presence of atrazine and 2,4-D (2, 4-Dichlorophenoxy acetic acid), respectively. The adsorption process was exothermic, driven by physisorption mechanisms like pore filling and electrostatic attraction. However, for an adsorbent to be ideal in real-time applications, rapid adsorption performance is crucial. The adsorbent attained equilibrium in 120 min, which could be considered as a limitation. By further modifying the adsorbent's surface with positively charged functional groups, a rapid adsorption reaction could be achieved through enhanced electrostatic interactions.

The conjugation of MOFs with CNTs has been shown to enhance pollutant removal due to their combined high surface area, porosity, and functionality. Specifically, ZIF-8 and UiO-66-NH_2 MOFs were modified on the polydopamine (PDA) functionalized MWCNT, creating an aerogel with remarkable hydrophilicity and thermal stability. This aerogel demonstrated high adsorption capacities for the herbicides chipton and alachlor, with maximum capacities of 160.9 and 246.8 mg g^{-1} for ZIF-8@MPCA, and 160.9 and 246.8 mg g^{-1} for UiO-66-NH_2@MPCA, respectively [98]. The adsorption is attributed to π-π stacking, hydrogen bonding, and electrostatic interaction. Biosafety assessment indicates that the aerogels did not release MOFs into the environment, suggesting low environmental risk (Fig. 4**b**). Additionally, a thorough investigation on the interference of other herbicides or some common metal ions should be conducted to prove the potential of developed adsorbents. In industrial applications, the use of fixed bed columns is practical for the removal of pollutants. A recent study demonstrated an approach involving the synthesis of magnetic-MWCNTs (CNT/Fe_3O_4) as adsorbents for the removal of pirimicarb, achieving a maximum adsorption efficiency of 101.3 mg g^{-1} [99]. The thermodynamics of adsorption revealed that the removal process is exothermic, involving both inter- and intra-particle diffusion mechanisms. These findings contribute to the understanding of the potential of magnetic-MWCNT as an efficient adsorbent for pesticide removal, particularly in industrial applications using fixed bed columns.

Activated carbon (AC)

Biochar and AC, sourced from biomass are carbon-rich materials, effective in removing agrochemicals from wastewater due to their hydrophobic nature and micro-porosity [100]. Phenoxy herbicides, commonly used in agrochemicals, pose environmental concerns by forming chlorophenol, which is linked to immune disorders [101]. To address their remediation, two commercially available ACs, GAB and CPB were used for removing 4-chloro-2-methyl phenoxy acetic acid (MCPA) and 2,4-D [101]. GAB and CPB exhibited SSA of 1189 m^2g^{-1} and 1288 m^2g^{-1}, respectively, and their microporous structures greatly enhanced adsorption, which was aided by π-π interactions and hydrogen bonding. The maximum adsorption capacities were 367.1519 mg g^{-1} for 2,4-D on GAB and 273.0683 mg g^{-1} on CPB, while for MCPA they were 599.8785 mg g^{-1} on GAB and 399.865 mg g^{-1} on CPB. However, the study lacks discussions on regeneration, long-term stability, and the impact of co-existing contaminants on the adsorption efficiency, which is crucial for practical applications and cost-effectiveness.

The use of biomass to produce biochar/AC for water remediation is highly attractive due to its cost-effectiveness [102]. In this scenario, the synthesis of AC by processing waste tangerine seeds with phosphoric acid (H_3PO_4) under high-temperature conditions to effectively remove carbamate pesticides from wastewater and plants was explored [103]. The resulting AC exhibited a SSA of 659.62 $m^2\ g^{-1}$ with a pore size of 1.41 nm, making it highly suitable for adsorption of six pesticides namely, bendiocarb, metolcarb, isoprocarb, pirimicarb, carbaryl, and methiocarb displaying a maximum adsorption capacity of 7.97, 9.11, 13.95, 39.37, 44.64, and 93.46 mg g^{-1}, respectively. The adsorption was attributed to hydrogen bonding and Van der Waal's forces. It's noteworthy that the physicochemical properties and adsorption efficacy of AC are intrinsically linked to the nature of the carbon source used in its production, exemplifying the significant impact of the chosen biomass waste on the performance of resulting material. In another study, queen palm fruit derived AC, activated with zinc chloride ($ZnCl_2$), had an even higher SSA of 782 $m^2\ g^{-1}$ and excellent at removing 2,4-D with an adsorption efficiency of 367.77 mg g^{-1} [104]. This adsorption process was achieved through the combination of hydrogen bonding, electrostatic, and π-π interactions. Notably, the synthesized AC proved durable, maintaining its adsorption capacity over seven cycles. Both studies underscore the importance of the biomass source in determining the AC's properties and effectiveness. However, further studies are needed to evaluate the interference of other contaminants and reusability for real-time applications. The findings suggest that the adsorption reactions are primarily due to weak physical interactions, which may affect the efficiency in real-time applications where samples may have multiple pollutants. Further altering the AC's surface with the different functional groups could enhance pollutant selectivity. Post-adsorption, separation of fine AC particles from water using common techniques like coagulation, and sedimentation is challenging. Introducing magnetic properties to the AC could offer a cost-effective and straightforward separation method using an external magnetic field.

In this regard, a magnetic-activated carbon composite was designed by combining manganese ferrite (MnF_2O_4) and AC using a solvothermal method, targeting acetochlor pesticides [105]. This composite displayed a SSA of 1287.3 $m^2\ g^1$ and a micropore volume of 0.3 $cm^3\ g^{-1}$, achieving an adsorption efficiency of 226 mg g^{-1}. In practical tests with wastewater, it demonstrated an adsorption rate of $>$ 75 %. The adsorption relied on several factors, including π-π interactions, hydrogen bonding, and pore filling. Moreover, the composite facilitated the degradation of acetochlor via a heat-activated peroxymonosulfate (PMS) oxidation process, achieving 90 % degradation efficiency with a PMS concentration of 9.6 mM at 70 °C within 12 h. However, the composite's low regeneration efficiency, due to the continuous destruction of the $MnFe_2O_4$@AC structure and deposition of intermediates was identified as a limitation. Enhancing the composite's stability could address this, making the simultaneous adsorption and degradation approach more effective for environmental remediation. This method could lead to the complete mineralization of pollutants into less harmful by-products, mitigating environmental risks.

Building on this concept, the study introduced an activated carbon (AC) fabric designed to remove the pesticide metaldehyde [106]. The fabric consists of many AC fibers forming a mesh-like structure with high porosity, offering a large surface area for wastewater treatment. It showed a removal efficiency of 1375 μg g^{-1} in lab conditions and 876 μg g^{-1} with real water sources. The micro-porous nature of the fibers is crucial for the rapid adsorption of metaldehyde. While promising at the lab scale, further testing and optimization of AC fabrics in highly permeable reactor configurations is necessary to assess its performance and robustness in continuous flow conditions. Also, the impact of multiple pesticides and their cross-interference must be investigated for practical applicability.

Graphene oxide (GO)

Recently, the use of functionalized graphene materials for the adsorption of pesticides from waste water has become increasingly popular. Graphene with its inherent stability, a high surface area,

abundant sp^2 hybridization, and extensively delocalized π–π electrons, has a strong affinity for adsorption, especially for pesticides that contain benzene rings [107]. In this context, a magnetic graphene-based nanocomposite, functionalized with N-methyl-D-glucamine calixarene (MGO-NGC) was developed to remove chlorinated pesticides namely, chlorpyrifos and hexaconazole [108]. Calixarene is a macrocyclic oligomer known for its three-dimensional cavity structure, which exhibits significant host-guest chemistry suggesting their potential as effective adsorbents [109,110]. The additional functionalization of calixarene with graphene has enhanced adsorption capacity and dispersibility in aqueous media achieving a removal efficiency over 80 % in 30 min, with adsorption capacities of 78.74 mg g^{-1} for chlorpyrifos and 93.4 mg g^{-1} for hexaconazole. This was attributed to the electrostatic interaction, π–π stacking, and hydrogen bonding. However, the study did not explore the interaction between GO, magnetic nanoparticle, and NGC. There is a possibility that magnetic nanoparticles might leach during NGC modification, which could affect the composite's stability and magnetic properties. Building on this concept, a study used rice husk waste to produce a magnetic GO functionalized with amino-guanidine, resulting in AGu@mGO formation [111]. This adsorbent demonstrated a removal efficiency of 90.39 % with an adsorption capacity of 85.47 mg g^{-1} for chlorpyrifos within 30 min. This efficient removal was achieved through π-π interactions and hydrogen bonds between the guanidine groups and the pesticide. However, the study lacks the impact of interfering compounds that might affect the adsorbent's performance. Therefore, it's crucial to note the practical limitations of previous methods, such as lengthy synthesis processes and the extensive use of chemicals. These challenges could be overcome by employing magnetic MOF and an in situ composite formation method, which could reduce the preparation time and quantity of chemicals used. MOFs, with their vast surface area, have the potential to adsorb large amounts of pollutants, thereby improving the stability and reusability of the adsorbents.

In recent years, advanced oxidation processes (AOPs) have emerged as efficient and practical alternatives to conventional treatment techniques for waste-water treatment [112]. This process involves versatile mechanisms that generate oxidizing reactive species (photocatalysis) [113]. The most common AOP, the Fenton process, utilizes Fe(II) ions and hydrogen peroxide (H_2O_2) to generate free ·OH radicals [114], which effectively mineralize persistent organic pollutants in water. In a study, a significant development was made with the synergistic use of amine-functionalized Fe_3O_4 wrapped GO (AFG) to support MIL-101 (Fe) (AFG@30MIL-101(Fe)) for the degradation of pesticides such as diazinon and atrazine (Fig. 5**a**) [115]. The composite achieved a degradation efficiency of 100 ± 1 % for diazinon and 81 ± 1 % for atrazine within 105 min. Graphene oxide's role as an electron acceptor and its ability to reduce charge carrier recombination significantly improved the photodegradation process, maintaining over 75 % efficiency after four cycles. However, the regeneration efficiency was lower for atrazine compared to diazinon, possibly due to stronger hydrogen bonds between the amide groups of atrazine and AFG@30MIL-101(Fe). Beside this, potential interference of other metal ions, pesticides and assessing the toxicity of the degradation by-products are crucial factors to be considered for future studies.

Considering the benefits of photocatalysis, a composite material comprising magnetite (GO-Fe_3O_4) and cobalt ferrite-decorated graphene oxide (GO-$CoFe_2O_4$) for the photocatalytic degradation of acetamiprid was developed [116]. To address agglomeration and low photocatalytic efficacy, GO was introduced into a metal ferrite structure. The acetamiprid degradation rates were 97 % for GO-$CoFe_2O_4$ and 90 % for GO-$Fe3O_4$ within an hour under UV-light. The catalyst's uniform dispersion ensures exposure of active sites to the oxidant and pesticide, with the composites maintaining over 65 % efficiency after five cycles.

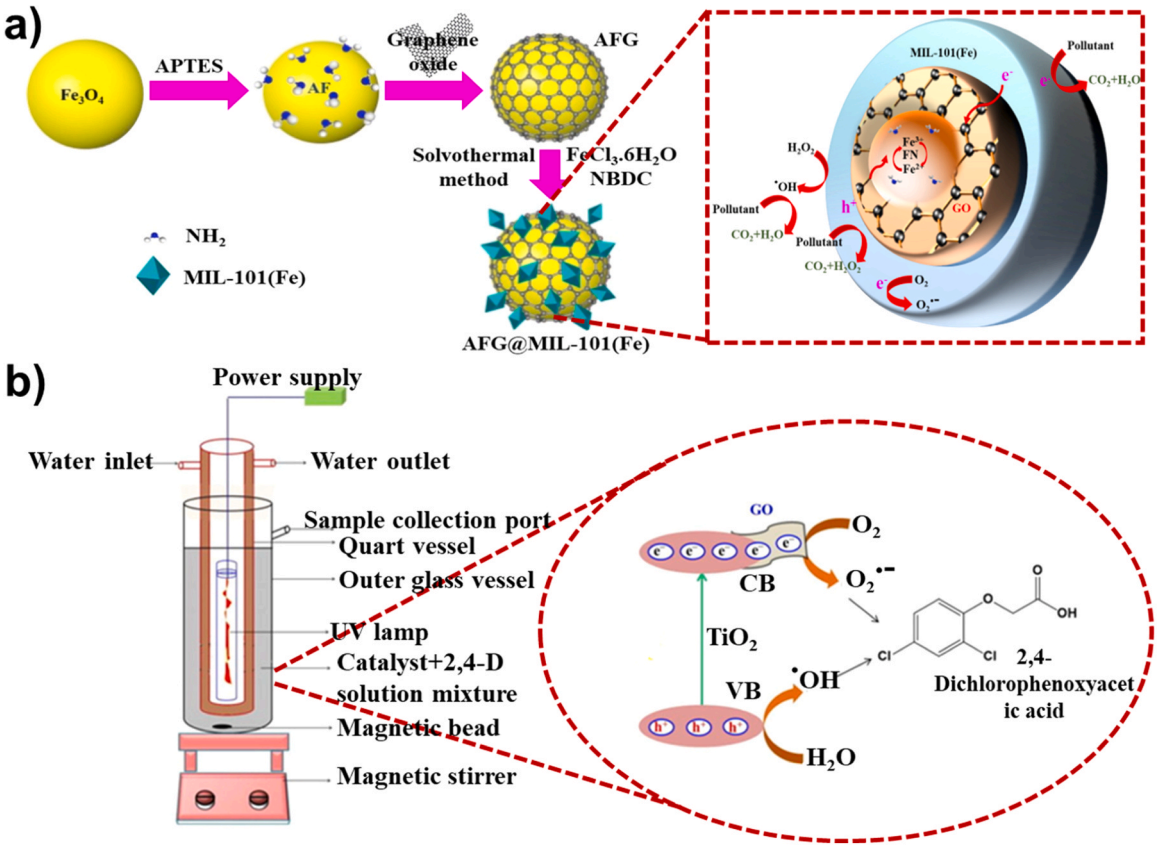

Fig. 5. Schematic representation of a) preparation of AFG@30MIL-101(Fe) through the solvothermal method and proposed degradation mechanism of diazinon and atrazine. b) Photoreactor for degradation reaction and separation mechanism of photo-generated electron-hole pairs on $TiO_2/GO_{7\,\%}$ under UV light.
(a) Printed with permission from Ref. [115]. Copyright 2020, Elsevier. (b) Printed with permission from Ref. [117]. Copyright 2021, Elsevier.

Further, a titanium oxide (TiO_2) and GO ($TiO_2/GO_{7\ \%}$) nanocomposite was investigated as a potent photocatalyst for degrading 2,4-D [117]. The integration of a heterojunction between the p-type semiconductor of GO and the n-type of TiO_2 improved charge carrier recombination rates, leading to 100 % degradation within 240 min. The process generates hydroxyl radicals and superoxide radical anions, which convert the herbicide into less harmful substances (Fig. 5b). However, the above studies focus on model pollutants, limiting the generalizability of the findings to other pesticides. Though photocatalysts have proven their effectiveness in pollutant degradation, there is ongoing debate regarding the toxicity analysis of intermediates generated during the degradation process. Additionally, a significant drawback of this approach is the lengthy time required by most photocatalysts to effectively degrade pollutants. Therefore, advancing photocatalysts with faster degradation rates is a key challenging task in the field.

The above findings highlight the potential of CNMs as effective adsorbents and catalysts for the remediation of a broad spectrum of contaminants through adsorption and degradation. CNM's high surface area and porosity provide numerous adsorption sites, enabling interactions with agrochemicals through physical and chemical mechanisms. Surface modification of CNMs improves their selectivity and affinity for specific agrochemicals, enhancing efficiency. While there are various strategies for pollution remediation, photocatalytic degradation stands out as an effective method that has so far received limited attention. In the case of photocatalysts, agrochemicals tend to concentrate on the surface of the adsorbent, which facilitates the degradation. Importantly, it sets itself apart from adsorption techniques by reducing the production of extensive sludge. Despite the numerous catalysts reported for the photodegradation of various organic pollutants, their practical application on a large scale or in real-world scenarios is often impeded by factors such as the spatial arrangement within crystal structures, particle sizes, and aggregation in solutions. By leveraging the properties of carbon-based photocatalysts, there is an opportunity to advance the field of photocatalytic degradation and pave the way for more sustainable methods of pollution remediation. Furthermore, the synergy between adsorption and degradation offers a holistic and efficient remediation approach, offering advantages in terms of selectivity and effectiveness. Carbon materials such as carbon dots, carbon quantum dots, and fullerenes, have not demonstrated adsorbent performance because of their limited surface area and porosity. Further, surface modification with functional groups or other nanomaterials could enhance the surface area which would help to achieve expected results in remediation.

Carbon nanomaterials for agrochemical delivery

In recent years, nanotechnology has emerged as a promising tool in agrochemical delivery [118], addressing plant diseases and crop protection while reducing the excessive use of agrochemicals. Recognized by the International Union of Pure and Applied Chemistry (IUPAC) in 2019 as one of the top ten chemical technologies, nano pesticides offer benefits such as comprehensive coverage, deep penetration, increased efficacy, reduced labor costs, and targeted absorption [119,120]. The integration of nanotechnology involves the use of NPs loaded with agrochemicals, which are applied directly to plants or soil, ensuring efficient and concentrated delivery (Fig. 6) [121]. This method not only improves the effectiveness of agrochemicals but also promotes sustainable farming practices.

NP-based pesticides and fertilizers are categorized into two main groups based on size and function. Category I encompasses NPs that are less than 100 nm in size and act as pesticides or fertilizers. Category II, on the other hand, consists of larger NPs ranging from 100 to 1000 nm in size, which are used as carriers for agrochemicals. CNMs have demonstrated their versatility capable of functioning as agrochemicals or as carriers for targeted delivery [122]. Moreover, CNMs have been shown to enhance plant growth, increase biomass, and improve seed germination [123]. They also play a crucial role in regulating nutrient intake and transport mechanisms, leading to improved uptake of essential nutrients like nitrogen and phosphorus by altering soil physicochemical

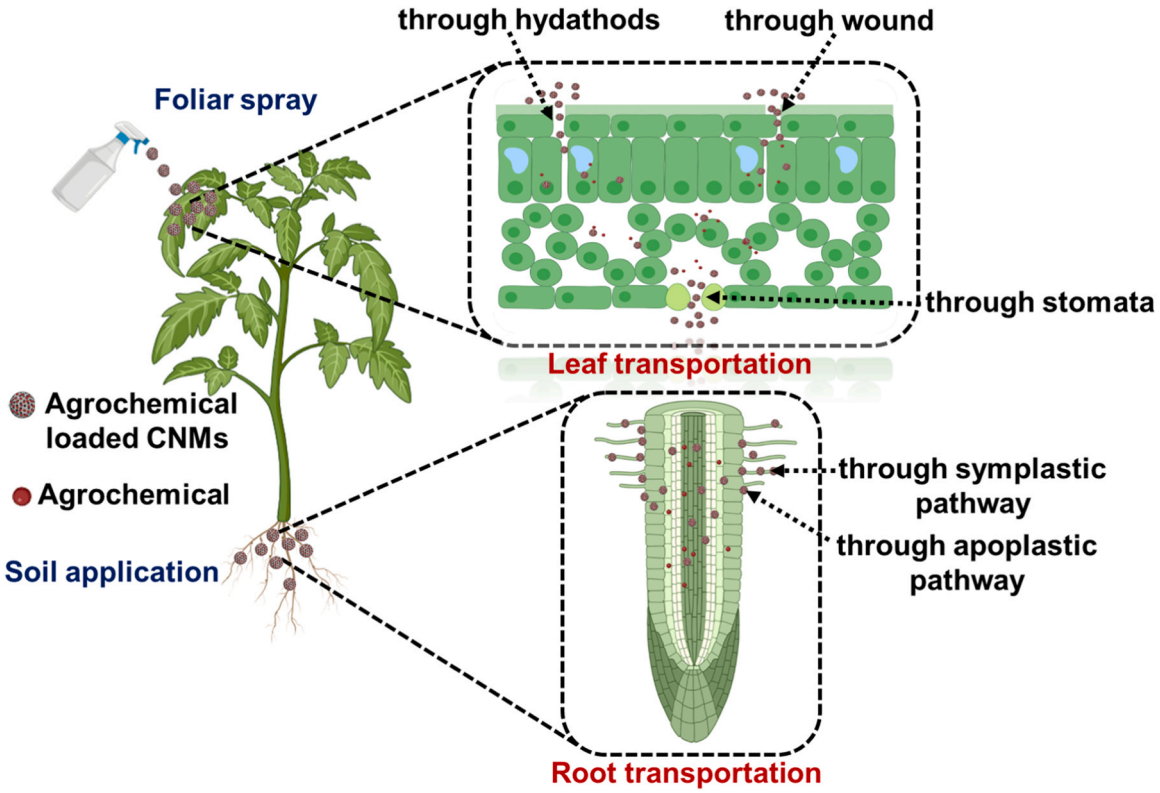

Fig. 6. Nanoparticle-mediated carriers for the controlled release of agrochemicals and their uptake mechanism by leaf and root.

characteristics [124].

Carbon nanotubes (CNTs)

CNTs have proven to be advanced nano-vectors for delivering agrochemicals effectively due to their large surface area and unique optical/electrical properties. They can be intricately linked with agrochemicals through non-covalent or covalent bonds, leading to the development of an innovative delivery system. In this context, pyraclostrobin pesticide was loaded onto MWCNTs (Pyr@MWCNT) through physisorption, achieving a drug loading capacity of 16.64 % [125]. The nano formulation released the pesticide gradually over 15 days, with a total release of 86.16 %. Additionally, Pyr@MWCNT demonstrated antifungal efficacy against *Pyricularia oryzae,* demonstrating an EC_{50} of 0.054 mg L^{-1}, comparable to the Pyr technical concentration. This indicates MWCNT's high efficiency in pesticide delivery and strong antifungal action. However, the use of bare carbon-based materials for agrochemical delivery may pose challenges, such as lower loading efficiency and the potential inability to deliver the required amount of agrochemicals to the intended site within the desired timeframe. To address these challenges, surface modification of nanocarriers emerges as a promising approach to enhance their properties, transforming them into smart cargo-carriers.

Activated carbon (AC)

AC and biochar are exceptional in adsorbing chemicals, making them ideal for agrochemical delivery due to their cost-effectiveness, eco-friendliness, and stability [126]. Their surfaces can be strategically modified to enhance electrostatic affinity, enhancing adsorption and release properties [127]. For instance, AC loaded with the herbicide 2, 4-D achieved a 67.91 % loading efficiency, attributed to its large surface area of 2248 m^2 g^{-1}. Despite this, 2,4-D was released within 96 h with a cumulative release of 32.21 %. To improve this, AC was modified with PDA followed by carbonization, creating N_2-doped AC (ACN) with activated pores but a lower loading efficiency of 21.50 %, likely due to pore blockage from the modifications [128]. Notably, ACN exhibited a controlled release profile, achieving a cumulative release of 48 % in 10 days which was driven by chemical interactions. Further research is needed to understand the release mechanisms, plant toxicity, impact on soil health, and antifungal properties of these nanocarriers. A recent study developed a controlled release system for the herbicide quinclorac (QNC) using biochar functionalized with γ-FeOOH nanoarrays (γ-FeOOH@BC) (Fig. 7**a**) [129]. The incorporation of the iron composite during the nanocarrier synthesis introduced numerous active sites for electrostatic interactions, resulting in a loading capacity of 90 mg g^{-1}. QNC's pH-dependent release behavior exhibited < 30 % release at lower pH and > 50 % at higher pH, reaching 88 % at pH 12 after 24 h (Fig. 7**b, c**). However, the assembly efficiency of QNC could decrease in

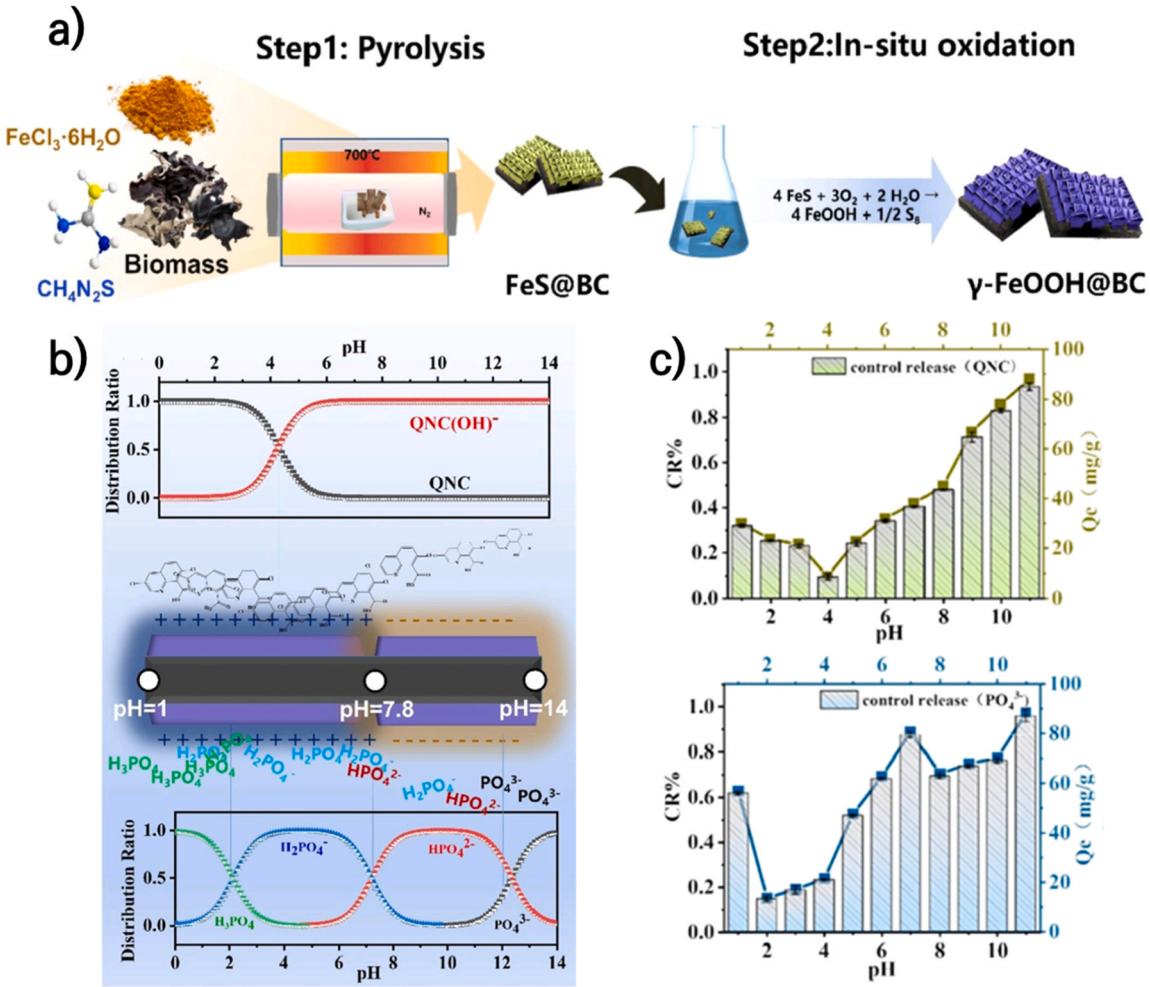

Fig. 7. Schematic representation of a) synthesis of γ-FeOOH@BC through pyrolysis of biomass followed by in-situ oxidation, b) Electrostatic self-assembly of quinclorac on γ-FeOOH@BC. c) Effect of pH on the release of QNC, and PO_4^{3-} by γ-FeOOH@BC.
Printed with permission from Ref. [129]. Copy Right 2022, Elsevier.

negatively charged soil and the dissolution, loss of γ-FeOOH, and oxidation of ferrous sulfide (FeS) were observed during the assembly process, raising concerns about the stability of the material. This can be mitigated by further modifying the carrier for better soil interaction and reducing γ-FeOOH consumption for improved stability.

Graphene oxide (GO)

Among the diverse nanocarriers developed for agrochemicals, GO stands out as a robust scaffold due to its advantageous features including easy surface modification, high loading capacity, large surface area, and excellent water dispersibility [130]. The presence of numerous oxygen groups on the surface of GO sheets renders [131] them a distinctive substrate for multivalent functionalization and effective loading of active substances. Since Dai et al.'s pioneering work in 2008, which introduced GO as a nanocarrier in drug delivery, there has been significant research into its use in biomedical fields, including gene delivery and plant biology [132]. GO's diverse capabilities highlight its potential to revolutionize agrochemical delivery systems, contributing to more effective and sustainable agricultural practices.

To explore the efficacy of GO for pesticide delivery, a nanocomposite was developed by decorating copper selenide (Cu_2Se) nanocrystals on the rGO surfaces for chlorpyrifos delivery [133]. The introduction of Cu_2Se provided photothermal properties to the nanocomposite. The nanocarrier showed a 40 % pesticide loading efficiency and an 80 % encapsulation efficacy, facilitated by strong π-π interactions and hydrogen bonding. It also displayed pH-responsive release, discharging 30 % under basic, 25 % under acidic, and 17 % under neutral conditions within 5 days. Additionally, photothermal release was observed with 17 % pesticide release within 7 min at 47 °C. The release behavior under the different pH conditions could be due to the susceptibility of hydrogen bonding to the pH change, where -COOH groups will turn into -COO (carboxylate). Meanwhile, the photothermal release suggested that the change in the binding energy of pesticide with composite material triggered the pesticide release, resulting in four times higher than without irradiation. Besides this, nanocomposites have a large hydrodynamic size of 820 nm, which may affect their dispersion and stability. These limitations could be addressed by adjusting the size of the material during the synthesis process. Further, to improve loading efficiency, polylactic acid-modified graphene oxide (PLA/GO) microspheres were developed for the extended release of Pyr [134]. These microspheres, with 0.5 % GO content in an acetone-chloroform solvent mixture, achieved a 39.89 % drug-loading capacity. In-vitro release study conducted over 30 days at temperatures of 30 °C, 40 °C, and 50 °C revealed release profiles of 51 %, 78 %, and 90 %, respectively. The microspheres also exhibited significant antifungal activity against *Rhizoctonia solani*, which was three times more effective than a commercial 9 % Pyr suspension. The sustained release of the Pyr was attributed to the combined effects of Pyr dispersion and matrix erosion within microspheres. The plant growth studies using 0.5 % GO demonstrated improved growth. However, the study did not explore the effect of pH on the release behavior. Given that pathogen infections in plants alter the pH of the infected area [135], it's expected that the developed nanocarriers would release active ingredients more effectively in the same pH condition. Furthermore, a GO-Pyr nanopesticide formulation showed antifungal activity against rape sclerotinia and wheat scab diseases caused by *Fusarium graminearum* and *Sclerotinia sclerotiorum* in the oilseed rape plants [136]. This nanocarrier exhibited a high loading capacity of 87.04 %, attributed to its large surface area and diverse functional groups. It released 50 % of Pyr within the initial 48 h, with a sustained release of 70 % in 168 h. However, the study lacked detailed in-vivo antifungal activity and long-term environmental impact assessment of GO-Pyr, which are crucial factors that could potentially limit their applicability. Incorporating stimuli-responsive materials such as lauric acid, PDA, and other capping agents, could allow for more controlled pesticide release.

Continuing with this, a GO-based nanocarrier was designed by grafting thermally sensitive poly(N-isopropylacrylamide) (PNIPAm) onto the GO surface for photothermal responsive release of insecticide lambda-cyhalothrin (LC) [137]. The nanocarrier had a 15.4 % loading efficiency and showed temperature-responsive release of 31.14 %, 44.54 %, and 54.99 % at 27 °C, 30 °C, and 35 °C, respectively, over 7 days. At 27 °C, the PNIPAm polymer shell expands and thickens, reducing insecticide release, and contracts at higher temperatures, increasing release. Despite the introduction of an intelligent stimuli-responsive release concept, the study has a few limitations such as poor loading efficiency and an early release of insecticide. This could be due to the PNIPAm polymer being initially grafted onto the GO surface, forming a layer-like structure on the GO surface that resulted in a lack of active sites for insecticide binding. These limitations can be addressed by first incorporating the insecticide onto the GO surface and then capping the nanocarrier with thermally sensitive materials. This approach would provide more active sites on the GO for insecticide, thereby enhancing the loading efficiency. Furthermore, the outer polymer layer could serve as a gatekeeper, ensuring controlled and extended release of insecticide. A recent study demonstrates the practical application of GO-insecticide nanocomposites against *Ostrinia furnacalis* [138]. In the nanocomposite formulation, GO was blended with insecticide, namely β-cyfluthrin (Cyf), monosultap (Mon), and imidacloprid (Imi), in a 2:1 ratio (insecticide: GO). The nanocomposite showed high insecticidal activity with mortality rates of 90 % for GO-Cyf (100 μg mL^{-1}), 80.1 % for GO-Mon (500 μg mL^{-1}), and 72.6 % for GO-Imi (1000 μg mL^{-1}). The observed mortality rates for nanocomposites were significantly higher than those for insecticides alone. The treatment with GO induced disruption and damage to the insect cement layer, leading to accelerated water loss and creating a pathway for insecticides to enter the insect's cuticle. At the same time, several key factors still need to be addressed to ensure its sustainable and safe design, including the toxic effect of GO on non-target organisms and the environmental risks associated with using GO for plant protection.

The limitations including low utilization efficiency and unstable characteristics of bifenthrin (Bif), fenpropathrin (Fen), and cyhalothrin (Cyh) insecticides have led to the development of GO-pesticide nanocomposites [139]. Insecticides were loaded onto the GO through the adsorption process bearing the loading capacities of 77.13 %, 122.10 %, and 74.03 % for Bif, Cyh, and Fen, respectively. Release tests in a methanol-water medium at 25 °C showed an initial burst release of 11 % in 2 h, followed by a cumulative release of 20 % over 168 h. At 30 °C, the release increased to nearly 40 % in the same duration. Notably, the nano-insecticide composite exhibited adsorption to spider mite cuticles, leading to the immobilization and potential disruption of vital physiological processes. Further, a commonly used insecticide, Emamectin benzoate (EB) is known for high efficacy, low toxicity, and impressive insecticidal activity. However, its practical use is hindered by several challenges, including low water solubility, rapid degradation, and issues with burst release. To address this, a GO-nanocarrier with polyethylene glycol (PEG) was created to enhance the EB's long-term stability for delivery [140]. The physisorption method for EB loading achieved 164.7 % loading capacity and a sustained release of 36.5 % over 10 days. The introduction of PEG into the materials not only increased their photostability but also enabled superior insecticidal performance even under intense sunlight conditions for 14 days. Further, by addressing the challenge of Abamectin (Abm) degradation under temperature, a controlled release system was developed by loading Abm onto a graphene-based nanocarrier [141]. The designed nano formulation exhibited enhanced water dispersion and stability over a 2-year storage period. Nanocarrier demonstrated an initial burst release within the first 2 h, succeeded by a cumulative release of 32 % over 10 days. Furthermore, Abm-GO nanoformulation showed toxicity against *Plutella xylostella*, while being less toxic to maize seedlings and reducing cytotoxicity to A549 cells.

Other carbon nanomaterials

Carbon nanoparticles (CNPs), derived from AC, offer outstanding water dispersibility, stability, and biocompatibility [142]. Their strong light absorption capability enhances the photoprotection of unstable molecules [142], leading to improved stability during therapeutic applications. Building on this, carboxymethyl chitosan-modified carbon NPs (CMC/CNPs) as a carrier for EB was developed (Fig. 8a,b,c) [143]. The nanocomposite exhibited a loading capacity of 55.56 % with a burst release of 10 % during the first 4 h, followed by a cumulative release of 44.5 % over 240 h at pH 7. The CMC/CNPs demonstrated pH-responsive behavior, releasing 76 % in acidic conditions due to protonated amines and CNPs swelling. In pest control tests against *Mythimna separata,* the nanocomposite achieved a death rate exceeding 60 % after 14 days. However, the study lacks a comprehensive analysis of the long-term impacts on environment and plants.

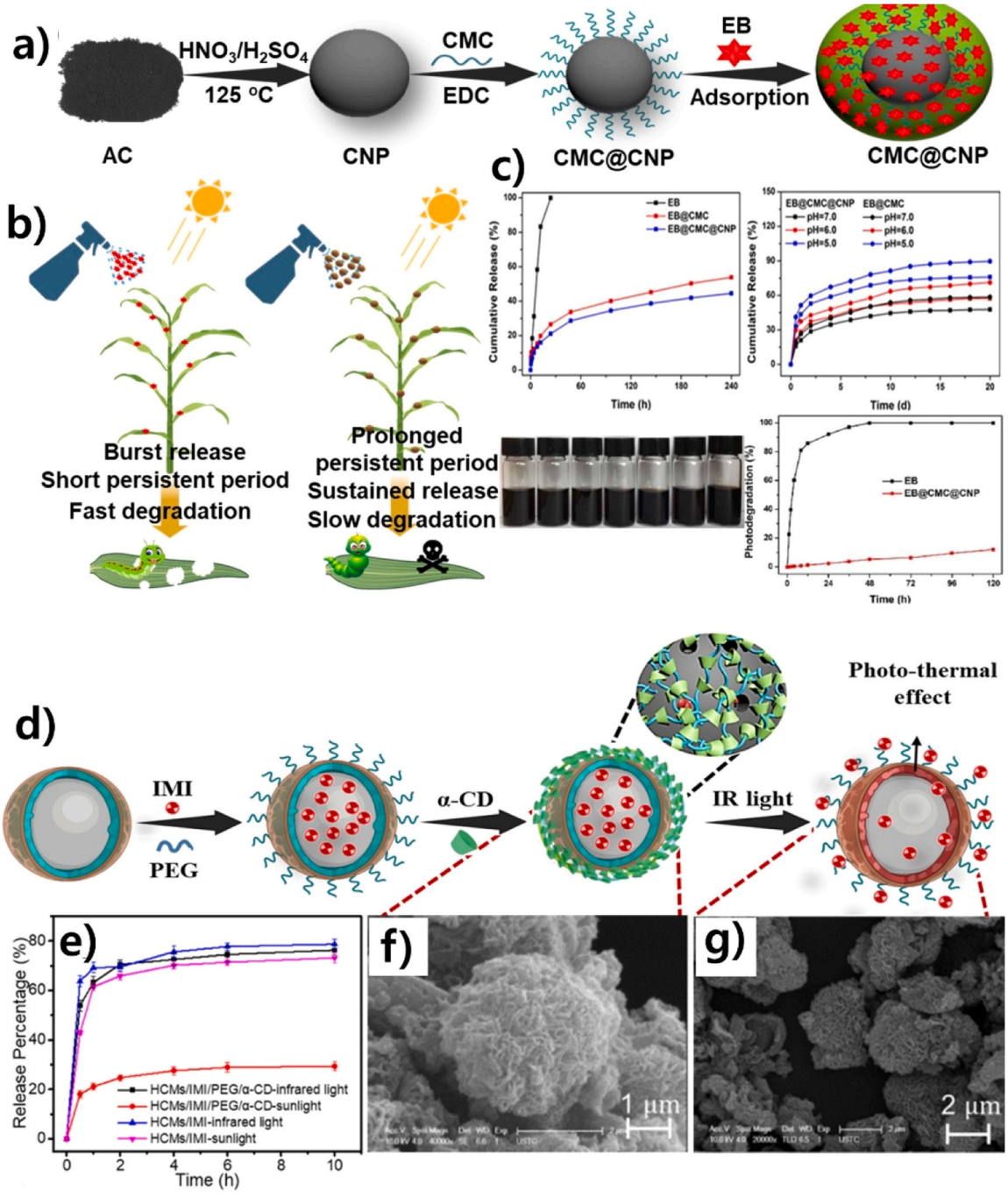

Fig. 8. Schematic representation of a) development of EB@CMC@CNP through fast oxidation, amidation reaction, and loading of insecticide through physical adsorption. b) Application of EB@CMC@CNP in insecticide release and sustainable pest control. c) Release performance of free EB, EB@CMC, and EB@CMC@CNP (pH 7.0), release performance of EB@CMC, and EB@CMC@CNP at pH 5.0, 6.0, and 7.0, photograph showing EB@CMC@CNP at one-year storage period, degradation rate of free EB and EB@CMC@CNP. d) Schematic representation of the development of HCM nanocarrier and IR-responsive release behavior of loaded pesticide. e) IR lamp and simulated sun light-responsive release of Imi, SEM images of f) HCMs/Imi/PEG/α-CD, g) HCMs/Imi/PEG/α-CD after Imi release.
(c) Printed with permission from Ref. [143]. Copyright 2019, American Chemical Society.(g) Printed with permission from Ref. [144]. Copyright 2021, American Chemical Society

Hollow carbon microspheres (HCM), a photothermal agent, were synthesized using calcium carbonate microspheres ($CaCO_3$) as a templet and dopamine as a carbon source [144]. Imidacloprid (Imi) was loaded into these HCMs, which were then coated with PEG and α-cyclodextrin (α-CD) to form a light-responsive delivery system (HCM/IMI/-PEG/α-CD) (Fig. 8d). The system features a gel-like network where PEG chains infiltrate α-CD cavities, acting as a capping layer that allows controlled release of 77 % Imi in response to IR light at 66.2 °C, while under normal sunlight, the release was 29 % (Fig. 8e). The heat generated by the Imi-loaded HCM under IR light disrupts the PEG/α-CD network, enabling the controlled release and targeted delivery of Imi. It's worth noting that the high temperature of the release system under the IR lamp could be a possible limitation of the study. Employing alternative thermal-sensitive materials like lauric acid could potentially allow for a release at a temperature range of ~44 °C [145].

Carbon nanomaterials for fertilizer delivery

Fertilizers are crucial ingredients in improving soil fertility and plant growth [146]. Over the past decades, several controlled-release fertilizer formulations have been developed to address the limitations of conventional fertilizers, such as high solubility, poor thermal stability, decreased soil fertility, and low nutrient efficiency [147]. Nitrogenous fertilizers are among the most significant micronutrients in agriculture, and often lead to inefficient plant nutrition due to the unstable nature of nitrogen in the form of nitrate or ammonium ions, resulting in low nitrogen uptake (NU) and nitrogen utilization efficiency (NUE). To improve this, MWCNTs were chemically activated with nitric acid to bond with the nitrogen from urea, creating UF-MWCNTs [148]. The 0.50 wt% UF-MWCNTs significantly enhanced nitrogen uptake to 1363 mg/pot and NUE to 96.35 % in paddy fields over 21 h. However, higher UF-MWCNT concentration and longer treatment time led to a decrease in the outcome. Further investigation is necessary to explore the impact of soil pH on release rate and long-term stability. The accumulation of UF-MWCNTs outside the plant organelles leads to the agglomeration of MWCNTs, damaging the organelles. Adjusting the size of MWCNTs may help them penetrate properly without accumulation.

Furthermore, a controlled-release fertilizer system was developed for urea granules encapsulated in biochar-crosslinked polymer films [149]. The films, made from polyvinyl alcohol (PVA) and polyvinylpyrrolidone (PVP), reduce water absorbency, which is crucial for nutrient release control. A soil column leaching study indicated a 65.28 % nitrogen release on the 22nd day, attributed to the film's less hydrophilic hydroxyl linkages and dense urea encapsulation. However, the biodegradability of PVA and PVP raises concerns for sustainable farming. To continue with, hydrogel-based formulations are recognized as effective release systems capable of holding large amounts of micronutrients and can progressively discharge them into the soil. With this regard, a hydrogel-based composite with pine resin biochar was designed for controlled micronutrient release namely, nitrogen (N), phosphorus (P), and potassium (K) [150]. The inclusion of biochar into the hydrogel matrix improved the water retention ability, porosity, and reduced bulk density of the carrier. In an aqueous medium, the presence of hydrophilic functional groups contributed to a high degree of swelling demonstrating a controlled release rate of $<$ 85 % in 12 days. Meanwhile, a 90 % release rate was achieved in soil due to the diffusion of micronutrients through small cracks and pores. The study did not explore the mechanical properties, plant absorption, or growth effects of these materials. Further, a study showed that biochar nanocarriers can effectively deliver urea to maize, with an initial release of 45–70 % in the first hour and continued slow release up to 72 h [151]. The leaching of nitrate (NO_3^-) into soil was significantly reduced, which decreased water contamination. The carrier improved the maize shoot (1–34 %), root (0–23 %) biomass, and N-recovery efficiency (17–50 %). However, further research on material analysis, loading efficiency, soil pH, temperature, and moisture-responsive release studies are required to understand their response under field conditions. Generally, fertilizers are proton donors and exist in different forms (molecular state, negative or positive ionic states) depending on the acidity of the environment. The pKa value of fertilizer phosphate (PO_4^{3-}) is 4.34, suggesting that they stay in anion form in the natural environment, and developing positively charged carriers would facilitate electrostatic self-assembly as well as pH-responsive control release. To explore this, positively charged γ-FeOOH functionalized biochar, with a phosphate loading capacity of 92 mg g^{-1}, has been used to enhance adhesion and enable pH-responsive release [129]. The developed carrier demonstrated a release rate of 13.68 % at pH 2, whereas 88 % release was observed at pH 11, suggesting the pH-responsive release behavior. The influence of temperature on release rate was observed which might be due to the faster molecular diffusion, achieving 92 % at 35 °C. Another study reported the development of a GO-Fe composite for phosphate (P) delivery with dual-release properties [152]. The result showed only 10 % of P was released during the first 10 h followed by a slow release for the next 40 h. The slow release was attributed to the strong complexation between trapped P and GO-Fe. The research indicates that the high solubility of monoammonium phosphate (MAP) leads to rapid transport in sandy soils and substantial P loss during leaching experiments, emphasizing the need for better fertilizer formulations to reduce environmental impact. Also, the kinetics of GO degradation in soil need further investigation to prevent potential toxicity issues associated with prolonged exposure, highlighting a gap in understanding the long-term effects of GO-based fertilizers on soil quality.

In conclusion, bare carbon materials tend to agglomerate in water due to strong Van der Waal interactions, leading to inadequate dispersion. Surface modification can improve the dispersibility of CNMs by enhancing their compatibility with solvents. Moreover, the development of stimuli-responsive nanocarriers has paved the way for improved controlled release systems. These nanocarriers can actively respond to signals or changes in their surroundings, such as variations in pH, temperature, light, or enzyme activity. Interestingly, graphene-based materials are majorly preferred for agrochemical delivery due to their high specific surface area, high dispersibility, electrostatic interactions, and π-π stacking, which enable efficient loading. These advancements in carbon-based nanocarriers offer promising prospects for more effective and sustainable agricultural practices.

Impact of CNMs on plant

The physical-chemical characteristics of NPs, such as concentration, surface charge, and particle size, are crucial in determining their biological effects on plants. While NPs can enhance plant growth and development [153], they can also be detrimental, affecting seed germination [154], seedling growth, and overall plant development [123]. Therefore, The interaction between NPs and living cells is vital for biosafety and the development of safer, more productive NP systems. Additionally, the development of NP systems that are less harmful and could boost crop output is crucial. Risks associated with NP exposure include DNA damage, changes in gene expression, and increased reactive oxygen species (ROS) [155], which vary depending on the plant species and NP properties [156]. For instance, CNTs can be harmful to tomato, rice, lettuce, and red spinach, causing cell death at certain concentrations, while benefiting tobacco cell growth. Even at a modest CNT dosage of 20 mg L^{-1}, rice plants experience cell chromatin condensation and membrane and cell wall separation, which causes the cells to shrink and eventually, lead to cell death [123]. In the case of GO, a high dose can inhibit plant growth and cause detrimental morphological alterations [157]. In addition, a study reveals that GO concentrations of roughly 50 mg L^{-1} boost superoxide dismutase (SOD) activity in plants, as well as H_2O_2, lipid, and protein oxidation, and reduce water absorption in seeds [158]. Other CNMs like fullerenes, and CQDs, also show some negative effects, including oxidative damage and reduced plant biomass [159], but can stimulate growth, cell division,

cell extension, gene expression, and improved water uptake [160]. Summarized from the reports, the potential risk of the CNMs on plant growth and development was found to be concentration-dependent and plant species-specific, highlighting the need for careful consideration in their application.

Future prospective

Though some of the CNMs are extensively used, certain types of CNMs such as modified CNTs, carbon dots, carbon nanohorns, and carbon spheres have not received significant attention in agriculture and environmental applications. Due to CNM's rapid detection capabilities, future research directions could focus on developing portable detection kits that assist farmers and researchers in the rapid on-site analysis of agrochemicals. Also, CNMs could be integrated with Internet of Things (IoT) technology, which could enable remote monitoring and data collection. Further, CNM's large surface area and porosity make them suitable for pollutant remediation, although issues like particle aggregation in CNTs and graphene in some cases exhibit less adsorption efficiency. In the future, these problems could be addressed, possibly by combining them with other nanomaterials to improve stability and reusability. These high surface area CNMs could be integrated with agriculture practices, employing them as filtration systems in irrigation, and nano-bioremediation systems using microorganisms to degrade the pollutants. In addition, carbon dot-based composite materials could be designed in such a way that they facilitate simultaneous adsorption and detection of pollutants. Although CNMs such as graphene and activated carbons are utilized as efficient agrochemical carriers, their environmental toxicity requires further study. Further research into modifying CNMs properties with proper functionalities and other eco-friendly materials, which could facilitate them to penetrate, translocate, and distribute in plant cellular levels is needed for precision delivery of active ingredients to reduce the possible environmental impact. This could provide insights into molecular-level interaction between CNMs and plants. Recently, the development of stimuli-responsive nanocarriers is gaining extensive interest. Thus, modifying CNMs by utilizing pH, enzyme, thermal, redox, and light-sensitive polymers/materials, could improve the shelf life of the agrochemicals and also facilitate precise delivery.

Conclusion

Recent advancements in carbon nanomaterials (CNMs) have witnessed remarkable outcomes in modern agriculture, particularly in agrochemical detection, remediation, and delivery. CNMs such as activated carbon (AC), carbon quantum dots (CQDs), multi-walled carbon nanotubes (MWCNTs), and graphene oxide (GO) are valued for their unique physical and chemical properties, which contribute to significant outcomes in the discussed studies. Their reactivity and cage-like structure offered promising avenues for selective agrochemical detection offering interactions between probes and analytes. Notably, attributes like rapid electron transfer, strong binding affinity, minimal residual current, and luminescent properties played crucial roles in enhancing detection methods. While addressing the environmental accumulation of agrochemicals, CNMs are also effective adsorbents due to their large surface area and porosity, offering simple synthesis and cost-effective solutions for large-scale applications. Additionally, the synergy between adsorption and photocatalytic activity contributes to advanced oxidation processes that minimize secondary waste in real-time remediation. In the field of delivering agrochemicals, high loading capacity, biocompatibility, facile synthesis, large surface area, and exceptional adsorption ability of CNMs make them excellent carriers, and their ability to be surface functionalized leads to the development of stimuli-responsive delivery systems. These nanocarriers have the potential to transform current agricultural practices into advanced technology aimed at improving the efficiency of agrochemical and nutrient delivery while minimizing negative environmental impact.

CRediT authorship contribution statement

Cheol Soo Kim: Writing – review & editing, Supervision. **Mahaveer D. Kurkuri:** Writing – review & editing. **Vinayak Hegde:** Writing – original draft, Conceptualization. **Kyeong-Hwan Lee:** Writing – review & editing, Supervision, Conceptualization. **Jae Ho Lee:** Writing – review & editing. **Mahesh P. Bhat:** Writing – review & editing, Supervision, Conceptualization.

Declaration of Competing Interest

The authors declare that they have no known competing financial interests or personal relationships that could have appeared to influence the work reported in this paper.

Data Availability

Data will be made available on request.

Acknowledgments

This work was supported by the Korea Institute of Planning and Evaluation for Technology in Food, Agriculture and Forestry (IPET) through the Open Field Smart Agriculture Technology Short-term Advancement Program, funded by the Ministry of Agriculture, Food and Rural Affairs (MAFRA) (32204003 and 32203703).

References

[1] G. HeiligFood security at different scales: demographic, biophysical and socio-economic considerations, 2025 (2025) 25.
[2] P.K.R. Maddikunta, S. Hakak, M. Alazab, S. Bhattacharya, T.R. Gadekallu, W. Z. Khan, Q.V. Pham, Ieee. Sens 21 (2021) 17608–17619, https://doi.org/10.1109/JSEN.2021.3049471.
[3] M.C. Hunter, R.G. Smith, M.E. Schipanski, L.W. Atwood, D.A. Mortensen, Bioscience 67 (2017) 386–391, https://doi.org/10.1093/biosci/bix010.
[4] A. Shahzad, S. Ullah, A.A. Dar, M.F. Sardar, T. Mehmood, M.A. Tufail, A. Shakoor, M. Haris, Environ. Sci. Pollut. Res. 28 (2021) 14211–14232, https://doi.org/10.1007/s11356-021-12649-8.
[5] G. Singh, K.K. Yogi, Asian J. Biol. Sci. 9 (2020) 274–285, https://doi.org/10.5530/ajbls.2020.9.42.
[6] P.A. Nazarov, D.N. Baleev, M.I. Ivanova, L.M. Sokolova, M.V. Karakozova, Acta Nat. 12 (2020) 46, https://doi.org/10.32607/actanaturae.11026.
[7] B.K. Singh, M. Delgado-Baquerizo, E. Egidi, E. Guirado, J.E. Leach, H. Liu, P. Trivedi, Nat. Rev. Microbiol. 21 (2023) 640–656, https://doi.org/10.1038/s41579-023-00900-7.
[8] S. Ali, A. Tyagi, H. Bae, Microorganisms 11 (2023) 392, https://doi.org/10.3390/microorganisms11020392.
[9] M. Junaid, A. Gokce, Bull. Biol. Allied Sci. Res. 2024 (2024), https://doi.org/10.54112/bbasr.v2024i1.66, 66-66.
[10] Y. Yapa, J.J. Wewalwela, Handbook of Agricultural Biotechnology, Nanofungicides, USA, 2024.
[11] A. Mandal, B. Sarkar, S. Mandal, M. Vithanage, A.K. Patra, M.C. Manna, Impact of agrochemicals on soil health. Agrochemicals Detection, Treatment and Remediation, Elsevier, 2020, pp. 161–187.
[12] C. An, C. Sun, N. Li, B. Huang, J. Jiang, Y. Shen, C. Wang, X. Zhao, B. Cui, C. Wang, X. Li, S. Zhan, F. Gao, Z. Zeng, H. Cui, Y. Wang, J. Nanobiotechnol. 20 (2022) 11, https://doi.org/10.1186/s12951-021-01214-7.
[13] T.O. Machado, S.J. Beckers, J. Fischer, B. Müller, C. Sayer, P.H.H. de Araújo, K. Landfester, F.R. Wurm, Biomacromolecules 21 (2020) 2755–2763, https://doi.org/10.1021/acs.biomac.0c00487.
[14] C.E. Okafor, I. Onyido, Sci. Rep. 12 (2022) 11169, https://doi.org/10.1038/s41598-022-15292-6.
[15] P. Shan, Y. Lu, W. Lu, X. Yin, H. Liu, D. Li, X. Lian, W. Wang, Z. Li, Z. Li, ACS Appl. Mater. Interfaces 14 (2022) 43759–43770, https://doi.org/10.1021/acsami.2c12106.
[16] H. Singh, A. Sharma, S.K. Bhardwaj, S.K. Arya, N. Bhardwaj, M. Khatri, Environ. Sci. Process. Impacts 23 (2021) 213–239, https://doi.org/10.1039/D0EM00404A.
[17] A. Aeron, E. Khare, C.K. Jha, V.S. Meena, S.M.A. Aziz, M.T. Islam, K. Kim, S. K. Meena, A. Pattanayak, H. Rajashekara, R.C. Dubey, B.R. Maurya, D. K. Maheshwari, M. Saraf, M. Choudhary, R. Verma, H.N. Meena, A.R.N. S. Subbanna, M. Parihar, S. Shukla, G. Muthusamy, R.S. Bana, V.K. Bajpai, Y.-K. Han, M. Rahman, D. Kumar, N.P. Singh, R.K. Meena, Arch. Microbiol. 202 (2020) 665–676, https://doi.org/10.1007/s00203-019-01779-w.

[18] A.S. Felsot, J.B. Unsworth, J.B.H.J. Linders, G. Roberts, D. Rautman, C. Harris, E. Carazo, J. Environ. Sci. Health B 46 (2010) 1–23, https://doi.org/10.1080/03601234.2010.515161.

[19] H.A. Yousef, H.M. Fahmy, F.N. Arafa, M.Y. Abd Allah, Y.M. Tawfik, K.K. El Halwany, B.A. El-Ashmanty, F.S. Al-anany, M.A. Mohamed, M.E. Bassily, Int. J. Trop. Insect Sci. 43 (2023) 1387–1399, https://doi.org/10.1007/s42690-023-01053-z.

[20] J. Luo, Y. Gao, Y. Liu, X. Huang, D.-x Zhang, H. Cao, T. Jing, F. Liu, B. Li, ACS Nano 15 (2021) 14598–14609, https://doi.org/10.1021/acsnano.1c04317.

[21] P. Rajput, A. Thakur, P. Devi, Emerging agrochemicals contaminants: current status, challenges, and technological solutions. Agrochemicals Detection, Treatment and Remediation, Elsevier, 2020, pp. 117–142, https://doi.org/10.1016/B978-0-08-103017-2.00005-2.

[22] S. Jiang, P. Li, L. Li, N. Amiralian, D. Rajah, Z.P. Xu, Green. Chem. 25 (2023) 8253–8265, https://doi.org/10.1039/D3GC02995F.

[23] R.A. Tessema, K. Nagy, B. Ádám, Int. J. Environ. Res. Public Health 18 (2021) 10431, https://doi.org/10.3390/ijerph181910431.

[24] D. Abdollahdokht, Y. Gao, S. Faramarz, A. Poustforoosh, M. Abbasi, G. Asadikaram, M.H. Nematollahi, Chem. Biol. Technol. Agric. 9 (2022) 13, https://doi.org/10.1186/s40538-021-00281-0.

[25] A. Acharya, P.K. Pal, NanoImpact 19 (2020) 100232, https://doi.org/10.1016/j.impact.2020.100232.

[26] S. Salazar Sandoval, T. Bruna, F. Maldonado-Bravo, P. Jara, N. Caro, C. Rojas-Romo, J. González-Casanova, D.R. Gómez, N. Yutronic, M. Urzúa, A. Rodríguez-San Pedro, Coatings 13 (2023) 2085, https://doi.org/10.3390/coatings13122085.

[27] L.F. Fraceto, R. Grillo, G.A. de Medeiros, V. Scognamiglio, G. Rea, C. Bartolucci, Front. Environ. Sci. 4 (2016) 186737, https://doi.org/10.3389/fenvs.2016.00020.

[28] Y. Ji, S. Ma, S. Lv, Y. Wang, S. Lü, M. Liu, ACS Appl. Mater. Interfaces 13 (2021) 43374–43386, https://doi.org/10.1021/acsami.1c11914.

[29] R.G. Moulick, S. Das, N. Debnath, K. Bandyopadhyay, Plant. Biotechnol. Rep. 14 (2020) 505–513, https://doi.org/10.1007/s11816-020-00636-3.

[30] A.N. Yadav, J. Appl. Biol. 9 (2021) 4, https://doi.org/10.7324/JABB.2021.94ed.

[31] A. Dhiman, A.K. Sharma, G. Agrawal, ACS Agric. Sci. Technol. 2 (2022) 693–711, https://doi.org/10.1021/acsagscitech.1c00278.

[32] R. Kumar, S. Ranjith, H. Balu, D.R. Bharathi, K. Chandan, S.S. Ahmed, UPI J. Pharm. Med. Health Sci. (2022) 39–43, https://doi.org/10.37022/jpmhs.v5i2.76.

[33] L.L. Mokoloko, R.P. Forbes, N.J. Coville, Nanomaterials 12 (2022) 2515, https://doi.org/10.3390/nano12152515.

[34] G. Speranza, C 5 (2019) 84, https://doi.org/10.3390/c5040084.

[35] S.F. Ahmed, P.S. Kumar, B. Ahmed, T. Mehnaz, G.M. Shafiullah, V.N. Nguyen, X. Q. Duong, M. Mofijur, I.A. Badruddin, S. Kamangar, Int. J. Hydrog. Energy 52 (2024) 424–442, https://doi.org/10.1016/j.ijhydene.2023.03.185.

[36] A.T. Krasley, E. Li, J.M. Galeana, C. Bulumulla, A.G. Beyene, G.S. Demirer, Chem. Rev. 124 (2024) 3085–3185, https://doi.org/10.1021/acs.chemrev.3c00581.

[37] S.J. Malode, S. Pandiaraj, A. Alodhayb, N.P. Shetti, ACS Appl. Bio. Mater. 7 (2024) 752–777, https://doi.org/10.1021/acsabm.3c00983.

[38] K. Piaskowski, P.K. Zarzycki, Int. J. Environ. Res. Public Health 17 (2020) 5862, https://doi.org/10.3390/ijerph17165862.

[39] M.S. Dresselhaus, M. Terrones, Proc. IEEE 101 (2013) 1522–1535, https://doi.org/10.1109/JPROC.2013.2261271.

[40] L.S. Porto, D.N. Silva, A.E.F. de Oliveira, A.C. Pereira, K.B. Borges, Rev. Anal. Chem. 38 (2019), https://doi.org/10.1515/revac-2019-0017.

[41] O. Zaytseva, G. Neumann, Chem. Biol. Technol. Agric. 3 (1) (2016) 26, https://doi.org/10.1186/s40538-016-0070-8.

[42] Y.-n Zhang, Q. Niu, X. Gu, N. Yang, G. Zhao, Nanoscale 11 (2019) 11992–12014, https://doi.org/10.1039/C9NR02935D.

[43] L.Y. Jun, N.M. Mubarak, M.J. Yee, L.S. Yon, C.H. Bing, M. Khalid, E.C. Abdullah, J. Ind. Eng. Chem. 67 (2018) 175–186, https://doi.org/10.1016/j.jiec.2018.06.028.

[44] R.K. Thines, N.M. Mubarak, S. Nizamuddin, J.N. Sahu, E.C. Abdullah, P. Ganesan, J. Ind. Eng. Chem. 72 (2017) 116–133.

[45] R. Thines, N. Mubarak, S. Nizamuddin, J. Sahu, E. Abdullah, P. Ganesan, J. Taiwan Inst. Chem. Eng. 72 (2017) 116–133, https://doi.org/10.1016/j.jtice.2017.01.018.

[46] Q. Zhao, Y. Lin, N. Han, X. Li, H. Geng, X. Wang, Y. Cui, S. Wang, Drug. Deliv. 24 (2017) 94–107, https://doi.org/10.1080/10717544.2017.1399300.

[47] G. Xu, S. Liu, H. Niu, W. Lv, RSC Adv. 4 (2014) 33986–33997, https://doi.org/10.1039/C4RA03993A.

[48] W.-R. Zhuang, Y. Wang, P.-F. Cui, L. Xing, J. Lee, D. Kim, H.-L. Jiang, Y.-K. Oh, J. Control. Release 294 (2019) 311–326, https://doi.org/10.1016/j.jconrel.2018.12.014.

[49] M. Saraji, M. Marzban, Anal. Bioanal. Chem. 396 (2010) 2685–2693, https://doi.org/10.1007/s00216-010-3496-z.

[50] C. Desmet, L.J. Blum, C.A. Marquette, Environ. Sci. Process. Impacts 15 (2013) 1876–1882, https://doi.org/10.1039/C3EM00296A.

[51] M. Badihi-Mossberg, V. Buchner, J. Rishpon, Electro (N.Y.) 19 (2007) 2015–2028, https://doi.org/10.1002/elan.200703946.

[52] P. Patil, Madhuprasad, M.P. Bhat, M.G. Gatti, S. Kabiri, T. Altalhi, H.-Y. Jung, D. Losic, M. Kurkuri, Chem. Eng. 327 (2017) 725–733, https://doi.org/10.1016/j.cej.2017.06.138.

[53] S. Chandra, D. Bano, K. Sahoo, D. Kumar, V. Kumar, P.K. Yadav, S.H. Hasan, Microchem. J. 172 (2022) 106953, https://doi.org/10.1016/j.microc.2021.106953.

[54] P.V. Mane, P. Patil, A.A. Mahishi, M. Kigga, M.P. Bhat, K.-H. Lee, M. Kurkuri, Heliyon 9 (2023) e16600, https://doi.org/10.1016/j.heliyon.2023.e16600.

[55] A.A. Mahishi, S.M. Shet, P.V. Mane, J. Yu, A.V. Sowriraajan, M. Kigga, M.P. Bhat, K.-H. Lee, M.D. Kurkuri, Anal. Methods 15 (2023) 3259–3267, https://doi.org/10.1039/D3AY00541K.

[56] M. Nehra, N. Dilbaghi, A.A. Hassan, S. Kumar, A. Deep, S. Kumar, Carbon-based nanomaterials for the development of sensitive nanosensor platforms, Adv. Nanosens. Biol. Environ. Anal. E-Publ. Inc. N. Y. (2019) 1–25, https://doi.org/10.1016/B978-0-12-817456-2.00001-2.

[57] N. Madima, S.B. Mishra, I. Inamuddin, A.K. Mishra, Environ. Chem. Lett. 18 (2020) 1169–1191, https://doi.org/10.1007/s10311-020-01001-0.

[58] D. Tyagi, H. Wang, W. Huang, L. Hu, Y. Tang, Z. Guo, Z. Ouyang, H. Zhang, Nanoscale 12 (2020) 3535–3559, https://doi.org/10.1039/C9NR10178K.

[59] G. Ponce-Vélez, G. de la Lanza-Espino, J. Environ. Prot. 10 (2019) 103–117, https://doi.org/10.4236/jep.2019.102007.

[60] Y. Nikmanesh, M. Farhadi, M. Taherian, P. Asban, F. Kiani, M.J. Mohammadi, Clin. Epidemiol. Glob. Health 25 (2024) 101508, https://doi.org/10.1016/j.cegh.2024.101508.

[61] A. Wong, T.A. Silva, F.R. Caetano, M.F. Bergamini, L.H. Marcolino-Junior, O. Fatibello-Filho, B. C. Janegitz C. 3 (2017) 8, https://doi.org/10.3390/c3010008.

[62] K. Jangid, R.P. Sahu, R. Pandey, R. Chen, I. Zhitomirsky, I.K. Puri, ACS Appl. Nano Mater. 4 (2021) 4781–4789, https://doi.org/10.1021/acsanm.1c00376.

[63] B. Yadav, S. Kaur, A. Yadav, H. Verma, S. Kar, B.K. Sahu, K.R. Pati, B. Sarkar, M. Dhiman, A.K. Mantha, J. Biochem. Mol. Toxicol. 38 (2024) e23660, https://doi.org/10.1002/jbt.23660.

[64] J.B. Thakkar, S. Gupta, C.R. Prabha, Int. J. Biol. Macromol. 137 (2019) 895–903, https://doi.org/10.1016/j.ijbiomac.2019.06.162.

[65] R. Liu, B. Li, F. Li, V. Dubovyk, Y. Chang, D. Li, K. Ding, Q. Ran, G. Wang, H. Zhao, Food Chem. 384 (2022) 132573, https://doi.org/10.1016/j.foodchem.2022.132573.

[66] C. Ding, A. Zhu, Y. Tian, Acc. Chem. Res. 47 (2014) 20–30, https://doi.org/10.1021/ar400023s.

[67] M.J. Molaei, Anal. Methods 12 (2020) 1266–1287, https://doi.org/10.1039/C9AY02696G.

[68] H. Xing, X. Wang, G. Sun, X. Gao, S. Xu, X. Wang, Environ. Toxicol. Pharmacol. 33 (2012) 233–244, https://doi.org/10.1016/j.etap.2011.12.014.

[69] S. Mohapatra, M.K. Bera, R.K. Das, Sens. Actuators B Chem. 263 (2018) 459–468, https://doi.org/10.1016/j.snb.2018.02.155.

[70] M. Veerappan, I. Hwang, M. Pandurangan, Int. J. Exp. Pathol. 93 (2012) 361–369, https://doi.org/10.1111/j.1365-2613.2012.00828.x.

[71] J. Liu, P. Zhang, Y. Zhao, H. Zhang, Ecotoxicol. Environ. Saf. 176 (2019) 242–249, https://doi.org/10.1016/j.ecoenv.2019.03.103.

[72] Y. Yang, X. Xing, T. Zou, Z. Wang, R. Zhao, P. Hong, S. Peng, X. Zhang, Y. Wang, J. Hazard. Mater. 386 (2020) 121958, https://doi.org/10.1016/j.jhazmat.2019.121958.

[73] X. Gong, Y. Wu, J. Li, S. Zhang, M. Wu, Carbon 226 (2024) 119208, https://doi.org/10.1016/j.carbon.2024.119208.

[74] M.K. Bera, L. Behera, S. Mohapatra, Colloids Surf. A Physicochem. Eng. Asp. 624 (2021) 126792, https://doi.org/10.1016/j.colsurfa.2021.126792.

[75] J. Liu, S. Bao, X. Wang, Micromachines 13 (2022) 184, https://doi.org/10.3390/mi13020184.

[76] D. Shahdeo, A. Roberts, N. Abbineni, S. Gandhi, Graphene based sensors. Compr. Anal. Chem, Elsevier, 2020, pp. 175–199, https://doi.org/10.1016/bs.coac.2020.08.007.

[77] A. Kumaravel, S. Aishwarya, S. Sathyamoorthi, Curr. Anal. Chem. 20 (2024) 383–409, https://doi.org/10.2174/0115734110294187240315082239.

[78] A. Pratap Singh Raman, G. Thakur, G. Pandey, K. Kumari, P. Singh, Chem. Biodivers. (2024) e202302080, https://doi.org/10.1002/cbdv.202302080.

[79] Z. Jin, W. Yim, M. Retout, E. Housel, W. Zhong, J. Zhou, M.S. Strano, J.V. Jokerst, Chem. Soc. Rev. (2024), https://doi.org/10.1039/D4CS00328D.

[80] L. Nana, L. Ruiyi, W. Qinsheng, Y. Yongqiang, S. Xiulan, W. Guangli, L. Zaijun, J. Hazard. Mater. 415 (2021) 125752, https://doi.org/10.1016/j.jhazmat.2021.125752.

[81] Y. Yao, G. Wang, G. Chu, X. An, Y. Guo, X. Sun, New. J. Chem. 43 (2019) 13816–13826, https://doi.org/10.1039/C9NJ02556A.

[82] B. McGleenon, K. Dynan, A. Passmore, Br. J. Clin. Pharmacol. 48 (1999) 471, https://doi.org/10.1046/j.1365-2125.1999.00026.x.

[83] M.K.L. da Silva, H.C. Vanzela, L.M. Defavari, I. Cesarino, Sens. Actuators B Chem. 277 (2018) 555–561, https://doi.org/10.1016/j.snb.2018.09.051.

[84] S. Tai, Q. Pan, X. Chen, C. Peng, C. Zhang, Z. Wang, Sens. Actuators B Chem. 378 (2023) 133130, https://doi.org/10.1016/j.snb.2022.133130.

[85] X. Zhang, W. Yan, J. Zhang, Y. Li, W. Tang, Q. Xu, RSC Adv. 5 (2015) 65532–65539, https://doi.org/10.1039/C5RA10 937J.

[86] L. Ma, L. Zhou, Y. He, L. Wang, Z. Huang, Y. Jiang, J. Gao, Biosens. Bioelectron. 121 (2018) 166–173, https://doi.org/10.1016/j.bios.2018.08.038.

[87] F.C. Vaz, T.A. Silva, O. Fatibello-Filho, M.H.M.T. Assumpção, F.C. Vicentini, Environ. Technol. Innov. 22 (2021) 101529, https://doi.org/10.1016/j.eti.2021.101529.

[88] K. Alagumalai, R. Shanmugam, S.M. Chen, B. Thirumalraj, A.S. Haidyrah, C. Karuppiah, Talanta 238 (2022) 123028, https://doi.org/10.1016/j.talanta.2021.123028.

[89] Y. Xia, Z. Xiao, Y. Yi, T. Liu, C. Zhang, G. Zhu, Microchem. J. 183 (2022) 108094, https://doi.org/10.1016/j.microc.2022.108094.

[90] P.I. Devi, M. Manjula, R. Bhavani, Annu. Rev. Environ. Resour. 47 (2022) 399–421, https://doi.org/10.1146/annurev-environ-120920-111015.

[91] F. Çeçen, Ö. AktaşActivated carbon for water and wastewater treatment: integration of adsorption and biological treatment, 1; 2011.
[92] K. Poonia, P. Singh, T. Ahamad, Q.V. Le, H.H. Phan Quang, S. Thakur, A. K. Mishra, R. Selvasembian, C.M. Hussain, V.-H. Nguyen, P. Raizada, Chemosphere 352 (2024) 141419, https://doi.org/10.1016/j.chemosphere.2024.141419.
[93] M. Sajid, M. Asif, N. Baig, M. Kabeer, I. Ihsanullah, A.W. Mohammad, J. Water Proc. Eng. 47 (2022) 102815, https://doi.org/10.1016/j.jwpe.2022.102815.
[94] G. Liu, L. Li, X. Huang, S. Zheng, X. Xu, Z. Liu, Y. Zhang, J. Wang, H. Lin, D. Xu, J. Mater. Sci. 53 (2018) 10772–10783, https://doi.org/10.1007/s10853-018-2352-y.
[95] A.M. Youssef, M.E. El-Naggar, F.M. Malhat, H.M. El Sharkawi, J. Clean. Prod. 206 (2019) 315–325, https://doi.org/10.1016/j.jclepro.2018.09.163.
[96] M.H. Dehghani, S. Kamalian, M. Shayeghi, M. Yousefi, Z. Heidarinejad, S. Agarwal, V.K. Gupta, Microchem. J. 145 (2019) 486–491, https://doi.org/10.1016/j.microc.2018.10.053.
[97] J.C. Diel, D.S.P. Franco, Id.S. Nunes, H.A. Pereira, K.S. Moreira, T.A. de, L. Burgo, E.L. Foletto, G.L. Dotto, J. Environ. Chem. Eng. 9 (2021) 105178, https://doi.org/10.1016/j.jece.2021.105178.
[98] W. Liang, B. Wang, J. Cheng, D. Xiao, Z. Xie, J. Zhao, J. Hazard. Mater. 401 (2021) 123718, https://doi.org/10.1016/j.jhazmat.2020.123718.
[99] M. Zahedinejad, N. Sohrabi, R. Mohammadi, J. Mol. Liq. 370 (2023) 120915, https://doi.org/10.1016/j.molliq.2022.120915.
[100] R.K. Gautam, M. Goswami, R.K. Mishra, P. Chaturvedi, M.K. Awashthi, R.S. Singh, B.S. Giri, A. Pandey, Chemosphere 272 (2021) 129917, https://doi.org/10.1016/j.chemosphere.2021.129917.
[101] A. Spaltro, M. Pila, S. Simonetti, S. Álvarez-Torrellas, J.G. Rodríguez, D. Ruiz, A. D. Compañy, A. Juan, P. Allegretti, J. Contam. Hydrol. 218 (2018) 84–93, https://doi.org/10.1016/j.jconhyd.2018.10.003.
[102] L. Campion, M. Bekchanova, R. Malina, T. Kuppens, J. Clean. Prod. 408 (2023) 137138, https://doi.org/10.1016/j.jclepro.2023.137138.
[103] Y. Wang, S.-l Wang, T. Xie, J. Cao, Bioresour. Technol. 316 (2020) 123929, https://doi.org/10.1016/j.biortech.2020.123929.
[104] Y.Ld.O. Salomón, J. Georgin, D.S.P. Franco, M.S. Netto, D.G.A. Piccilli, E. L. Foletto, L.F.S. Oliveira, G.L. Dotto, J. Environ. Chem. Eng. 9 (2021) 104911, https://doi.org/10.1016/j.jece.2020.104911.
[105] Y. Wang, C. Lin, X. Liu, W. Ren, X. Huang, M. He, W. Ouyang, Sci. Total Environ. 778 (2021) 146353, https://doi.org/10.1016/j.scitotenv.2021.146353.
[106] S. Cosgrove, B. Jefferson, P. Jarvis, Sci. Total Environ. 815 (2022) 152626, https://doi.org/10.1016/j.scitotenv.2021.152626.
[107] K.-Y. Andrew Lin, W.-D. Lee, J. Chem. Eng. 284 (2016) 1017–1027, https://doi.org/10.1016/j.cej.2015.09.075.
[108] H.R. Nodeh, M.A. Kamboh, W.A. Wan Ibrahim, B.H. Jume, H. Sereshti, M. M. Sanagi, Environ. Sci.: Process. Impacts 21 (2019) 714–726, https://doi.org/10.1039/C8EM00530C.
[109] M.A. Kamboh, I.B. Solangi, S.T.H. Sherazi, S. Memon, Desalination 268 (2011) 83–89, https://doi.org/10.1016/j.desal.2010.10.001.
[110] M.A. Kamboh, I.B. Solangi, S. Sherazi, S. Memon, J. Hazard. Mater. 186 (2011) 651–658, https://doi.org/10.1016/j.jhazmat.2010.11.058.
[111] V. Mahdavi, F. Taghadosi, F. Dashtestani, S. Bahadorikhalili, M.M. Farimani, L. Ma'mani, A. Mousavi Khaneghah, J. Environ. Chem. Eng. 9 (2021) 106117, https://doi.org/10.1016/j.jece.2021.106117.
[112] M. Priyadarshini, I. Das, M.M. Ghangrekar, L. Blaney, J. Environ. Manag. 316 (2022) 115295, https://doi.org/10.1016/j.jenvman.2022.115295.
[113] N. Nadeem, M. Zahid, A. Tabasum, A. Mansha, A. Jilani, I.A. Bhatti, H.N. Bhatti, Mater. Res. Express 7 (2020) 015519, https://doi.org/10.1088/2053-1591/ab66e.
[114] J. Tang, B. Hou, J. Liu, R. Deng, C. Wang, Z. Li, Y. Jiao, J. Environ. Chem. Eng. 12 (2024) 112666, https://doi.org/10.1016/j.jece.2024.112666.
[115] H. Fakhri, M. Farzadkia, R. Boukherroub, V. Srivastava, M. Sillanpää, Sol. Energy 208 (2020) 990–1000, https://doi.org/10.1016/j.solener.2020.08.050.
[116] A. Tabasum, M. Alghuthaymi, U.Y. Qazi, I. Shahid, Q. Abbas, R. Javaid, N. Nadeem, M. Zahid, Plants 10 (2020) 6, https://doi.org/10.3390/plants10010006.
[117] T.S. Natarajan, P.K. Gopi, K. Natarajan, H.C. Bajaj, R.J. Tayade, Water Energy Nexus 4 (2021) 103–112, https://doi.org/10.1016/j.wen.2021.07.001.
[118] D.Y. Kim, A. Kadam, S. Shinde, R.G. Saratale, J. Patra, G. Ghodake, J. Sci. Food Agric. 98 (2018) 849–864, https://doi.org/10.1002/jsfa.8749.
[119] S.N. Raj, E. Anooj, K. Rajendran, S. Vallinayagam, J. Mol. Struct. 1239 (2021) 130517, https://doi.org/10.1016/j.molstruc.2021.130517.
[120] D. Wang, N.B. Saleh, A. Byro, R. Zepp, E. Sahle-Demessie, T.P. Luxton, K.T. Ho, R. M. Burgess, M. Flury, J.C. White, Nat. Nanotechnol. 17 (2022) 347–360, https://doi.org/10.1038/s41565-022-01082-8.
[121] S.J. Beckers, A.H.J. Staal, C. Rosenauer, M. Srinivas, K. Landfester, F.R. Wurm, Adv. Sci. 8 (2021) 2100067, https://doi.org/10.1002/advs.202100067.
[122] S. Sharma, B.K. Sahu, L. Cao, P. Bindra, K. Kaur, M. Chandel, N. Koratkar, Q. Huang, V. Shanmugam, Prog. Mater. Sci. 121 (2021) 100812, https://doi.org/10.1016/j.pmatsci.2021.100812.
[123] S. Samadi, B. Asgari Lajayer, E. Moghiseh, S. Rodríguez-Couto, Environ. Technol. Innov. 21 (2021) 101323, https://doi.org/10.1016/j.eti.2020.101323.
[124] F. Zhao, X. Xin, Y. Cao, D. Su, P. Ji, Z. Zhu, Z. He, Nanomater 11 (2021) 2717, https://doi.org/10.3390/nano11102717.
[125] Y. Wang, J. Tian, Z. Wang, C. Li, X. Li, ACS Agric. Sci. Technol. 2 (2022) 534–545, https://doi.org/10.1021/acsagscitech.1c00293.
[126] Y. Dai, N. Zhang, C. Xing, Q. Cui, Q. Sun, Chemosphere 223 (2019) 12–27, https://doi.org/10.1016/j.chemosphere.2019.01.161.
[127] M.N. Nguyen, J. Clean. Prod. 307 (2021) 127188, https://doi.org/10.1016/j.jclepro.2021.127188.
[128] J. Yang, W. Zang, Z. Zhang, P. Wang, Q. Yang, Materials 12 (2019) 4019, https://doi.org/10.3390/ma12234019.
[129] Y. Wang, Z. Peng, Y. Yang, Z. Li, Y. Wen, M. Liu, S. Li, L. Su, Z. Zhou, Y. Zhu, N. Zhou, J. Chem. Eng. 437 (2022) 134984, https://doi.org/10.1016/j.cej.2022.134984.
[130] K. Chaudhary, K. Kumar, P. Venkatesu, D.T. Masram, Adv. Colloid Interface Sci. 289 (2021) 102367, https://doi.org/10.1016/j.cis.2021.102367.
[131] B. Gupta, N. Kumar, K. Panda, V. Kanan, S. Joshi, I. Visoly-Fisher, Sci. Rep. 7 (2017) 45030, https://doi.org/10.1038/srep45030.
[132] S. Kabiri, F. Degryse, D.N.H. Tran, R.C. da Silva, M.J. McLaughlin, D. Losic, ACS Appl. Mater. Interfaces 9 (2017) 43325–43335, https://doi.org/10.1021/acsami.7b07890.
[133] S. Sharma, S. Singh, A.K. Ganguli, V. Shanmugam, Carbon 115 (2017) 781–790, https://doi.org/10.1016/j.carbon.2017.01.075.
[134] Y. Wang, C. Li, T. Wang, X. Li, X. Li, Langmuir 36 (2020) 12336–12345, https://doi.org/10.1021/acs.langmuir.0c02320.
[135] D. Xiao, H. Wu, Y. Zhang, J. Kang, A. Dong, W. Liang, J. Control. Release 352 (2022) 288–312, https://doi.org/10.1016/j.jconrel.2022.10.028.
[136] F. Peng, X. Wang, W. Zhang, X. Shi, C. Cheng, W. Hou, X. Lin, X. Xiao, J. Li, Nanomater 12 (2022) 1112, https://doi.org/10.3390/nano12071112.
[137] Y. Wang, S. Song, X. Chu, W. Feng, J. Li, X. Huang, N. Zhou, J. Shen, Colloids Surf. A Physicochem. Eng. Asp. 612 (2021) 125987, https://doi.org/10.1016/j.colsurfa.2020.125987.
[138] X. Wang, H. Xie, Z. Wang, K. He, D. Jing, Environ. Sci. Nano. 6 (2019) 75–84, https://doi.org/10.1039/C8EN00902C.
[139] X. Gao, F. Shi, F. Peng, X. Shi, C. Cheng, W. Hou, H. Xie, X. Lin, X. Wang, RSC Adv. 11 (2021) 36089–36097, https://doi.org/10.1039/D1RA06505J.
[140] S. Song, M. Wan, W. Feng, J. Zhang, H. Mo, X. Jiang, H. Shen, J. Shen, ACS Agric. Sci. Technol. 1 (2021) 182–191, https://doi.org/10.1021/acsagscitech.1c00002.
[141] J. Liu, Y. Luo, X. Jiang, G. Sun, S. Song, M. Yang, J. Shen, Pest Manag. Sci. 78 (2022) 5358–5365, https://doi.org/10.1002/ps.7158.
[142] S. Song, H. Shen, T. Yang, L. Wang, H. Fu, H. Chen, Z. Zhang, ACS Appl. Mater. Interfaces 9 (2017) 9484–9495, https://doi.org/10.1021/acsami.7b00490.
[143] S. Song, Y. Wang, J. Xie, B. Sun, N. Zhou, H. Shen, J. Shen, ACS Appl. Mater. Interfaces 11 (2019) 34258–34267, https://doi.org/10.1021/acsami.9b12564.
[144] B. Liu, J. Zhang, C. Chen, D. Wang, G. Tian, G. Zhang, D. Cai, Z. Wu, J. Agric. Food Chem. 69 (2021) 6981–6988, https://doi.org/10.1021/acs.jafc.1c01265.
[145] M. Zare, K.S. Mikkonen, Adv. Funct. Mater. 33 (2023) 2213455, https://doi.org/10.1002/adfm.202213455.
[146] W. Dikr, K. Belete, Acad. Res. J. Agric. Sci. Res. 5 (2017) 192–204, https://doi.org/10.14662/ARJASR2017.016.
[147] A. Yadav, K. Yadav, K.A. Abd-Elsalam, Agrochemicals 2 (2023) 296–336, https://doi.org/10.3390/agrochemicals2020019.
[148] N.M. Yatim, A. Shaaban, M.F. Dimin, N. Mohamad, F. Yusof, Adv. Nat. Sci Nanosci. Nanotechnol. 10 (2019) 015011, https://doi.org/10.1088/2043-6254/ab0881.
[149] S. Chen, M. Yang, C. Ba, S. Yu, Y. Jiang, H. Zou, Y. Zhang, Sci. Total Environ. 615 (2018) 431–437, https://doi.org/10.1016/j.scitotenv.2017.09.209.
[150] S.K. Das, G.K. Ghosh, Energy 242 (2022) 122977, https://doi.org/10.1016/j.energy.2021.122977.
[151] C. Banik, S. Bakshi, D.A. Laird, R.G. Smith, R.C. Brown, J. Environ. Qual. 52 (2023) 630–640, https://doi.org/10.1002/jeq2.20468.
[152] S. Kabiri, I.B. Andelkovic, R.C. da Silva, F. Degryse, R. Baird, E. Tavakkoli, D. Losic, M.J. McLaughlin, Ind. Eng. Chem. Res. 59 (2020) 5512–5524, https://doi.org/10.1021/acs.iecr.0c00403.
[153] S.K. Verma, A.K. Das, S. Gantait, V. Kumar, E. Gurel, Sci. Total Environ. 667 (2019) 485–499, https://doi.org/10.1016/j.scitotenv.2019.02.409.
[154] U. Aqeel, T. Aftab, M.M.A. Khan, M. Naeem, M.N. Khan, Chemosphere 291 (2022) 132672, https://doi.org/10.1016/j.chemosphere.2021.132672.
[155] P.P. Fu, Q. Xia, H.-M. Hwang, P.C. Ray, H. Yu, J. Food Drug. Anal. 22 (2014) 64–75, https://doi.org/10.1016/j.jfda.2014.01.005.
[156] O. Zaytseva, G. Neumann, Chem. Biol. Technol. Agric. 3 (2016) 17, https://doi.org/10.1186/s40538-016-0070-8.
[157] P. Begum, R. Ikhtiari, B. Fugetsu, Carbon 49 (2011) 3907–3919, https://doi.org/10.1016/j.carbon.2011.05.029.
[158] Y. Yang, R. Zhang, X. Zhang, Z. Chen, H. Wang, P.C.H. Li, Plants 11 (2022) 2826, https://doi.org/10.3390/plants11212826.
[159] Y. Li, X. Xu, Y. Wu, J. Zhuang, X. Zhang, H. Zhang, B. Lei, C. Hu, Y. Liu, Mater. Chem. Front. 4 (2020) 437–448, https://doi.org/10.1039/C9QM00614A.
[160] M.H. Lahiani, J. Chen, F. Irin, A.A. Puretzky, M.J. Green, M.V. Khodakovskaya, Carbon 81 (2015) 607–619, https://doi.org/10.1016/j.carbon.2014.09.095.

Mr. Vinayak Hegde received bachelor's degree in Science from Karnataka University, Dharwad. He also earned a Master of Science degree in Chemistry from Centre for Nano and Material Sciences, Jain University, India. He is currently pursuing Ph.D. at the Department of Convergence Biosystems Engineering, Chonnam National University, Republic of Korea, under the supervision of Prof. Kyeong Hwan-Lee, where his research focus on the development of nano platforms for agrochemicals delivery in plants.

Prof. Kyeong Hwan-Lee is a professor at Department of Convergence Biosystems Engineering and Adjunct professor at Department of Intelligent Mobility and Department of Artificial Intelligence Convergence, Chonnam National University, Republic of Korea. He is the director of Agricultural Automation Research Centre, Sensors and Intelligent Biosystems Laboratory, and Fully-automated Digital Agriculture Complex Project. He is a member of Chonnam Local Government Committee on Science and Technology. He completed his Ph.D. at Dept. of Biological and Agricultural Engineering, Kansas State University, USA (2005). His research is focuses on Computer Vision and Robotics for Agriculture, Nanoscale Drug Delivery System for Agriculture, Digital Agriculture.

Dr. Mahesh P. Bhat, currently working as Research Professor at College of Agriculture and Life Sciences, Chonnam National University, South Korea under the supervision of Prof. Kyeong Hwan-Lee. He obtained Ph.D. in Chemistry from Centre for Nano and Material Sciences, Jain University, India in 2021. He has completed Master of Science in Analytical Chemistry from Mangalore University. During his Ph.D., he has worked on chemical sensors for environmental monitoring. His current research interests includes nano-scale agrochemical delivery systems, nanosensors, enviornmantal remediation.